Article Title

An improved *Nicotiana benthamiana* strain for aphid and whitefly research

Running title

Acylsugars protect *Nicotiana benthamiana*

Author names

Honglin Feng[1], Lucia Acosta-Gamboa[2], Lars H. Kruse[3], Alba Ruth Nava Fereira[4], Sara Shakir[1†], Hongxing Xu[1‡], Garry Sunter[4], Michael A. Gore[2], Gaurav D. Moghe[3], Georg Jander[1*]

Author Affiliations

[1]Boyce Thompson Institute, Ithaca NY, USA

[2]Plant Breeding and Genetics Section, School of Integrative Plant Science, Cornell University, Ithaca NY, 14853, USA

[3]Plant Biology Section, School of Integrative Plant Science, Cornell University, Ithaca NY, 14853, USA

[4]Department of Biology, University of Texas San Antonio, San Antonio TX, 78249, USA

[†]Present address: Gembloux Agro-Bio Tech Institute, the University of Liege, Gembloux, Belgium

[‡]Present address: College of Life Science, the Shaanxi Normal University, Xi'an, China

***Correspondence:**

Georg Jander

Boyce Thompson Institute

Ithaca, NY 14853

USA

Phone: 607-254-1365

Email: gj32@cornell.edu

Abstract

Nicotiana benthamiana is used extensively as a platform for transient gene expression and as a model system for studying plant-virus interactions. However, many tobacco-feeding insects, e.g. *Myzus persicae* (green peach aphids) and *Bemisia tabaci* (whiteflies), grow poorly on *N. benthamiana*, limiting its utility for research on plant-insect interactions. Using CRISPR/Cas9, we generated knockout mutations in two *N. benthamiana* acylsugar acyltransferase genes, *ASAT1* and *ASAT2*, which contribute to the biosynthesis of insect-deterrent acylsucroses. Whereas *ASAT1* mutations reduced the abundance of two predominant acylsucroses, *ASAT2* mutations caused almost complete depletion of foliar acylsucroses. Both *M. persicae* and *B. tabaci* survived and reproduced significantly better on *asat2* mutant plants than on wildtype *N. benthamiana*. Furthermore, *ASAT1* and *ASAT2* mutations reduced the water content and increased the temperature of leaves, indicating that foliar acylsucroses can protect against desiccation. Improved aphid and whitefly performance on *ASAT2* mutants will make it possible to use the efficient transient overexpression and gene expression silencing systems that are available for *N. benthamiana* to study plant-insect interactions. Additionally, the absence of acylsugars in *ASAT2* mutant lines will simplify transient expression assays for the functional analysis of acylsugar biosynthesis genes from other Solanaceae.

Introduction

Nicotiana benthamiana, a species of wild tobacco that is native to Australia, is commonly used by plant molecular biologists as model system for laboratory research. Susceptibility to a wide variety of plant viruses has made *N. benthamiana* a popular model for fundamental studies of plant-virus interactions (Goodin et al., 2008; Bally et al., 2018). Scientists have developed *N. benthamiana* as a transgene expression powerhouse by engineering viral vectors to express heterologous genes, including fluorescent reporter genes to visualize cell structures (Bally et al., 2018). Antibodies, biofuel compounds, and other protein and metabolite products have been produced in *N. benthamiana* (Arntzen, 2015; Powell, 2015). Virus-induced gene silencing (VIGS), which is employed to study gene function in a variety of plant species, was originally developed in *N. benthamiana* (Hayward et al., 2011). Recently, high-efficiency CRISPR/Cas9 germline gene editing using virus-encoded guide RNA (gRNA) was demonstrated for the first time in *N. benthamiana* (Ellison et al., 2020). Although *N. benthamiana* is hyper-susceptible to many plant viruses, it is not a good host for two virus-transmitting Hemiptera, *Myzus persicae* (green peach aphid) (Thurston, 1961; Hagimori et al., 1993) and *Bemisia tabaci* (silverleaf whitefly) (Simon et al., 2003), that grow well on cultivated tobacco (*Nicotiana tabacum*).

The poor growth of aphids and whiteflies on *N. benthamiana* may be attributed in part to glandular trichomes. These epidermal secretory structures on the leaf surface of ~30% of vascular plants (Weinhold and Baldwin, 2011; Glas et al., 2012), have been found to play a crucial defensive role in several ways: as a physical obstacle for insect movement on the plant surface (Cardoso, 2008), entrapment (Simmons et al., 2004), production of volatiles and other defensive metabolites (Laue et al., 2000; Schilmiller et al., 2010; Glas et al., 2012), and production of proteins that repel herbivores (phylloplane proteins, e.g. T-phylloplanin) (Shepherd and Wagner, 2007). In addition to their defensive functions, glandular trichomes also protect plants from abiotic stresses such as transpiration water loss and UV irradiation (Karabourniotis et al., 1995).

There are two main types of glandular trichomes on *N. benthamiana* leaves, large swollen-stalk trichomes and small trichomes that are capped by a secretory head with one, two, or four cells (Slocombe et al., 2008). The large trichomes have been shown to secrete phylloplane proteins in *N. tabacum*. The small trichomes are the most abundant trichomes on tobacco leaf surfaces and secrete exudates, including acylsugars (Wagner et al., 2004; Slocombe et al., 2008). Detached trichomes, a mixture of the large and small trichomes, from *N. benthamiana* are able to synthesize acylsugars (Kroumova and Wagner, 2003), and the secretory head cells alone are able to synthesize acylsugars in *N. tabacum* (Kandra and Wagner, 1988).

Acylsugars, generally sucrose or glucose esterified with aliphatic acids of different chain lengths, are abundant insect-deterrent metabolites produced by Solanaceae glandular trichomes (Arrendale et al.,

1990; Slocombe et al., 2008; Moghe et al., 2017). Specific acylsugars are associated with aphid-resistant *Nicotiana* species, while not being detected in more susceptible species in this genus (Hagimori et al., 1993). Furthermore, relative to cultivated tomatoes (*Solanum lycopersicum*), acylsugars provide wild tomatoes (*Solanum pennellii*) greater resistance against *M. persicae* (Rodriguez et al., 1993). Diacylsucrose protects crops against tobacco aphids (*Myzus persicae nicotianae*), *B. tabaci*, and two-spotted spider mites (*Tetranychus urticae*) (Chortyk et al., 1996; Alba et al., 2009). The synthetic sucrose octanoate (an analog of *Nicotiana gossei* sugar esters) is effective in the field against Asian citrus psyllids (*Diaphorina citri*), citrus leafminer (*Phyllocnistis citrella*), and a mite complex (including Texas citrus mite, red spider mite, and rust mite) (McKenzie and Puterka, 2004). Interestingly, acylsucroses in *Nicotiana attenuata* are metabolized to volatile fatty acids by neonate *Manduca sexta* (tobacco hornworm) larvae, thereby tagging these larvae and attracting predatory ants, *Pogonomyrmex rugosus* (Weinhold and Baldwin, 2011).

Acylsugars and leaf surface lipids more generally may contribute to plant drought tolerance. Transcriptomic studies of drought tolerant wild tomato (*Solanum pennellii*) populations showed that lipid metabolism genes are among those that are most responsive to drought stress (Gong et al., 2010; Egea et al., 2018). Additionally, acylsugars on the leaf surface in a native *S. pennellii* population contributed to drought tolerance (Fobes et al., 1985). Acylsugars also are reported to provide protection against drought stress conditions in *Solanum chilense* (O' Connell et al., 2007). Similarly, abundant accumulation of acylsugars with C7-C8 acyl groups the in the desert tobacco (*Nicotiana obtusifolia*) was suggested to provide this species with high drought tolerance for its desert environment (Kroumova et al., 2016). Although the mechanism is not completely understood, it has been proposed that the polar lipids reduce the surface tension of adsorbed dew water, thereby allowing the leaves absorb more condensed water on the surface (Fobes et al., 1985).

More recently, enzymes involved in the biosynthesis of acylsugars have been identified. Four acylsugar acyltransferases (ASATs), SlycASAT1, SlycASAT2, SlycASAT3, and SlycASAT4, have been biochemically characterized in cultivated tomato (Fan et al., 2016). SlycASAT1 catalyzes the first step of sucrose acylation, using sucrose and acyl-CoA to generate monoacylsucroses via pyranose R_4 acylation (Fan et al., 2016). SlycASAT2 uses the product of SlycASAT1 (e.g. S1:5(iC5^{R4})) and acyl-CoA donor substrates (*e.g.* iC4-CoA, aiC5-CoA, nC10-CoA, and nC12-CoA) to generate diacylsucroses (Fan et al., 2016). Further, SlycASAT3 uses the diacylsucroses generated by SlycASAT2 to make triacylsucroses by acylating the diacylsucrose five-membered (furanose) ring (Fan et al., 2016). Then, SlycASAT4 makes tetraacylsucroses by acetylating triacylsucroes using C2-CoA (Schilmiller et al., 2012). Notably, SlycASAT4 (formerly SlycASAT2) is specifically expressed in the trichomes, where acylsugar acetylation occurs (Schilmiller et al., 2012). The expression and activity of ASATs varies among different

plant species (including the order of the ASAT reactions in the pathway), which may contribute to the observed trichome chemical diversity (Kim et al., 2012). Although ASATs have been most intensively studied in tomato, *ASAT* genes also have been annotated in the available *Nicotiana* genomes (Gaquerel et al., 2013; Van et al., 2017; Egan et al., 2019). However, *ASAT* genes in *N. benthamiana* have not been annotated and characterized previously, and their functions in defense against insect pests remained unknown.

The goal of this study was to investigate the role of acylsugars in *N. benthamiana* resistance to insect feeding, as well as to create an insect-susceptible *ASAT* mutant line to facilitate use of *N. benthamiana* for laboratory research on plant-insect interactions. Here, we identified two *ASAT* genes in *N. benthamiana*, *NbenASAT1 and NbenASAT2*. Using CRISPR/Cas9 to create mutant lines, we showed that both *NbenASAT1* and *NbenASAT2* mutants had reduced acylsugar content. *NbenASAT2* mutations allowed increased *M. persicae* and *B. tabaci* survival, growth, and reproduction. Additionally, decreased water content and elevated leaf temperature in *NbenASAT1* and *NbenASAT2* mutants indicated that *N. benthamiana* acylsugars contribute to protection against desiccation.

Results

Identification of ASAT1 *and* ASAT2 *in N. benthamiana*

Using reciprocal comparisons to confirmed Solanaceae *ASAT* genes (Moghe et al., 2017), we identified three highly homologous sequences in the *N. benthamiana* genome: Niben101Scf02239Ctg025, Niben101Scf22800Ctg001, and Niben101Scf14179Ctg028 (Bombarely et al., 2012) (gene identifiers are from annotations at solgenomics.net). While Niben101Scf02239Ctg025 and Niben101Scf22800Ctg001 were annotated as a full-length coding sequences with strong coverage in available RNAseq datasets, Niben101Scf14179Ctg028 was annotated as a pseudogene because it appears to be a fragment of Niben101Scf141790g02010.1, with no coverage in available RNAseq datasets. The Niben101Scf02239Ctg025 and Niben101Scf22800Ctg001 sequences were confirmed in a more recently assembled *N. benthamiana* genome (Schiavinato et al., 2019). In this assembly, the pseudogene Niben101Scf14179Ctg028 was annotated as part of Niben101Scf02239Ctg025, and there were no additional annotated ASAT candidates.

To infer ASAT evolution and function, we constructed a protein phylogenetic tree of previously annotated Solanaceae ASATs (Figure 1, Figure S1; Table S1). In this tree, Niben101Scf02239Ctg025 formed a monophyletic group with other ASATs, including the biochemically characterized *Ssin*ASAT1, *Paxi*ASAT1 and *Hnig*ASAT1. Therefore, we named Niben101Scf02239Ctg025 as *N. benthamiana* ASAT1 (*Nben*ASAT1). Niben101Scf22800Ctg001 formed a monophyletic group with other ASATs including the biochemically characterized *Natt*ASAT2, *Hnig*ASAT2, and *Paxi*ASAT2. Therefore, we named Niben101Scf22800Ctg001 as *N. benthamiana* ASAT2 (*Nben*ASAT2). Notably, the ASAT2 monophyletic group also included the biochemically characterized *Spen*ASAT1, *Slyc*ASAT1, and *Snig*ASAT1 (Figure 1).

Generation of ASAT *mutants*

Using CRISPR/Cas9 coupled with tissue culture, we obtained two independent homozygous mutants for both *NbenASAT1* and *NbenASAT2*. *asat1-1* has a five-nucleotide deletion at the gRNA3 cutting site and a single nucleotide insertion at the gRNA2 cutting site, leading to a frameshift between gRNA3 and gRNA2. *asat1-2* has a 318-nucleotide deletion between the gRNA3 and gRNA2 cutting sites (Figure 2A). *asat2-1* has a single-nucleotide deletion at the gRNA3 cutting site and single-nucleotide insertion at the gRNA2 cutting site, leading to a translation frame shift between the two sites. *asat2-2* has a 115-nucleotides deletion at gRNA3 cutting site and a single-nucleotide insertion at the gRNA2 cutting site (Figure 2B).

ASAT2 *knockout depletes acylsugar biosynthesis*

We quantified the acylsugar content in the *ASAT* mutants by LC/MS, comparing to that of wildtype plants. In the LC/MS profile of *N. benthamiana* leaf surface washes, we characterized twelve mass features as acylsucroses based on their characteristic peaks and neutral losses (Figure S2A). In a negative electron spray ionization mode, the characteristic peak features included the mass of 341.11 for sucrose, 509.22 for sucrose + C2+C8, 467.21 for sucrose + C8, 495.21 for sucrose + C7, and 383.12 for sucrose + C2; the neutral loss peaks included mass for 126.10 for C8 (acyl-chain with 8 carbons), 129.09 for C7 + H_2O, and 59.01 for C2 + H_2O (Figure S2B). Those twelve *m/z* ratios included 383.12, 467. 21, 509.22, 555.23, 593.32, 621.31, M625.31, 635.32, 639.32, 667.32, 671.30, 681.34 (Figure S2A). Based on their MS/MS peak features, retention times and relative abundances, we predicted that the identified mass features are mainly derived from two acylsucroses as formate or chloride adducts, pathway intermediates and/or have resulted from in-source fragmentation. We named the two acylsucroses S3:17(2,7,8) and S3:18(2,8,8) (in the nomenclature, "S" refers to the sucrose backbone, "3:18" indicates three acyl chains with total eighteen carbons, and the length of each acyl chain is shown in parentheses) (Figure S2A). In wildtype plants, S3:18(2,8,8) is the dominant acylsucrose while S3:17(2,7,8) has relatively low abundance (Figure 3). S2:16(8,8) and S2:15(7,8), which may be biosynthetic pathway intermediates for S3:18(2,8,8) and S3:17(2,7,8), respectively, are present at lower levels (Figure 3). Compared to wildtype, both *asat2-1* and *asat2-2* were almost completely depleted in both acylsucroses (Figure 3). For *asat1-1* and *asat1-2*, the detected acylsucroses were less abundant, and significantly reduced in *asat1-1* (Figure 3). Although acylsugar content was significantly reduced in *ASAT* mutants, the structure and abundance of trichomes on the leaf surface were not changed (Figure S3).

Insect performance on ASAT2 *mutant lines*

We used *ASAT1* and *ASAT2* mutant lines to test the role of acylsugars in protecting *N. benthamiana* against aphid pests. The *ASAT2* mutations significantly improved *M. persicae* survival compared to both wildtype *N. benthamiana* and plants with *ASAT1* mutations (Figure 4A, S4A). Significant improvements in aphid performance were observed as early as at 48 h post-feeding ($p < 0.05$) and increased until the end of the 120-h monitoring period ($p < 0.001$) (Figure 4A, S4A). At the end of the survivorship assay, aphids on both *ASAT1* and *ASAT1* mutants were larger than those on wildtype plants (Figure 4B, S4B). When we measured progeny production by five adult aphids over a period of seven days, more than 200 nymphs were produced on the *ASAT2* mutants, significantly more than the number of nymphs produced on either wildtype or *ASAT1* mutants ($p < 0.05$, Figure 4C, S4C). In aphid choice assays with detached leaves, aphids preferentially chose *ASAT2* mutant leaves relative to wildtype and *ASAT1* mutants ($p < 0.05$, Figure 4D, S4D). This preference was consistently observed in pairwise choice assays in any combination between *ASAT2* mutants and either wildtype or *ASAT1* mutants ($p < 0.001$, *t*-test, Figure S5). No

preference was observed when comparing wildtype *N. benthamiana* and *ASAT1* mutants ($p > 0.05$, Figure 4D, S4D, S5).

When aphid colonies were allowed to grow long-term on *asat2-1* mutant and wildtype *N. benthamiana* in the same growth chamber, there were many more aphids on the mutant plants (Figure S6A,B), likely resulting from a combination of host plant choice and increase growth on the *asat2-1* mutant. It is noteworthy that, on the *asat2-1* mutant plants, aphids were feeding on the more nutritious younger leaves, but on the wildtype plants they only were able to feed on older leaves. Consistent with the increased aphid presence, growth of the *asat2-1* mutants was visibly reduced relative to wildtype *N. benthamiana* (Figure S6B).

To determine whether depletion of acylsugars in *ASAT2* mutants improves the performance of other insects on *N. benthamiana*, we conducted experiments with *B. tabaci*, *Heliothis virescens* (tobacco budworm) and *Trichoplusia ni* (cabbage looper). Survival of *B. tabaci* was greatly increased on the *asat2-1* mutant line relative to wildtype (Figure 5A and S6C). Moreover, whereas no eggs were observed on wildtype *N. benthamiana, B. tabaci* on *asat2-1* plants laid 0.42 +/- 0.15 eggs per adult in the course of the three-day experiment. After 23 days of feeding, whiteflies of different life stages were observed on *asat2-1* mutant plants including eggs, nymphs, and adults (Figure S6D-F).

Survivorship of *H. virescens* and *T. ni* larvae on *N. benthamiana* was low and the mass of the surviving larvae after ten days was not significantly increased on the mutant line relative to wildtype (Figure 5B,C). The size of the surviving larvae was about ten-fold smaller than what we have observed when these species were feeding on *N. tabacum* for a similar amount of time, and neither *H. virescens* nor *T. ni* larvae survived until pupation. In a repeat of this experiment with 16 replicates, only four *H. virescens* larvae survived for ten days on *asat2-1* and none survived on wildtype *N. benthamiana*. No *T. ni* survived on either *asat2-1* or wildtype plants.

ASAT2 mutant plants lose water faster than wildtype plants

While investigating the *ASAT* mutants, we noticed that the mutant plants dried out faster than wildtype plants. This effect was quantified using detached-leaf assays, in which leaves from *ASAT2* mutants lost significantly more water over 24 h than leaves from either wildtype or *ASAT1* mutants (Figure 6A, S7A). When plants are subjected to drought, high/low temperature, salinity, herbivores, or other stresses, they absorb and reflect specific wavelengths of light, which have been used to determine vegetation indices. For example, the water band index (WBI) (Penuelas et al., 1993) has been used to monitor changes in the plant canopy/leaf water content. Using hyperspectral imaging, we determined that the leaf water content of intact plants, as measured by the WBI, was significantly lower in *ASAT2* mutants than in wildtype (Figure 6B, S7B). Although the *ASAT1* mutants did not lose water faster than wildtype in detached leaf

assays (Figure 6A), the leaf water content in *ASAT1* mutants was significantly lower than wildtype (Figure 6B, S7B). Measurement of leaf temperature by thermal imaging showed that, consistent with the reduced leaf water content, the leaf temperature of the *asat1-1*, *asat2-1*, and *asat2-2* mutants was significantly higher than that of wildtype plants (Figure 6C, S7C). The temperature change in the *asat1-2* mutant was not significant at the $p < 0.05$ level (Figure 6C, S7C).

Discussion

We were able to identify only two *ASAT* genes, *NbenASAT1* and *NbenASAT2*, as well as a fragmented pseudogene, in the *N. benthamiana* genome (Table S1). By contrast, in other *Nicotiana* species, there are larger numbers of predicted *ASATs*, *e.g.* one *ASAT1*, one *ASAT2*, and 20 *ASAT3*-like genes in *N. attenuata* (Gaquerel et al., 2013; Van et al., 2017), 35 *ASAT3*-like genes in *N. tabacum*, and 19 *ASAT3*-like genes in *N. tomentosiformis* (Egan et al., 2019). Given the relatively small number of predicted *ASAT* genes in *N. benthamiana*, other enzymes may also be involved in acylsugar biosynthesis. In Solanaceae plants, two common pathways are known for aliphatic acid elongation via acetate: the fatty acid synthase (FAS) and the alpha-ketoacid elongation (αKAE) pathways (Kroumova and Wagner, 2003). In the FAS pathways, two carbons from an acetyl-acyl carrier are retained per elongation cycle, whereas in the αKAE pathway, one carbon is retained per elongation cycle (Kroumova and Wagner, 2003). The knockdown of *E1-β branched-chain α-keto acid dehydrogenase* (*BCKD*) significantly reduces acylsugars in *N. benthamiana* (Slocombe et al., 2008). In addition, *Isopropylmalate Synthase 3* (*IPMS3*) in cultivated and wild tomatoes (Ning et al., 2015) and *Acyl-Sucrose Fructo-Furanosidase 1* (*ASFF1*) in wild tomato (Leong et al., 2019) are involved in determining acylsugar composition. Further studies will be needed to characterize other genes involved in the *N. benthamiana* acylsugar biosynthesis pathway.

Acylsugars can be categorized as sucrose or glucose esters based on the sugar cores, which is decorated with varying numbers or lengths of acyl chains (Kim et al., 2012). Whereas some wild tomatoes produce a mixture of acylsucroses and acylglucoses, we only identified acylsucroses, consistent with previous identification of these compounds in *N. benthamiana* (Matsuzaki et al., 1989; Matsuzaki et al., 1992; Hagimori et al., 1993; Slocombe et al., 2008). Nevertheless, it has been reported that *N. benthamiana* produces acylglucoses, although in a smaller proportion/abundance than acylsucroses (Hagimori et al., 1993), and one glucose ester structure has been proposed (Matsuzaki et al., 1992). Our failure to detect acylglucoses may be explained by the growth conditions, growth stage of plants, and/or the LC/MS methods used. Whereas we used ~1-month old plants and LC/MS, Matsuzaki *et al.* used ~3-month old plants and GC/MS to detect acylglucoses in *N. benthamiana* (Matsuzaki et al., 1992).

Acylsugars with $C_{7\text{-}12}$ chains have been shown to be the most toxic sugar esters for small phloem-feeding arthropods such as aphids, Asian citrus psyllids, and whiteflies (Chortyk et al., 1996; McKenzie and Puterka, 2004; Song Z et al., 2006). Synthetic acylsucroses with di-heptanoic acid (C7), di-octanoic acid (C8), and di-nonanoic acid (C9) acyl groups showed the highest mortality in bioassays with *M. persicae* and *B. tabaci* (Chortyk et al., 1996; McKenzie and Puterka, 2004; Song Z et al., 2006). *Nicotiana gossei*, a tobacco species that produces mainly C7-C8 acyl group acylsugars, has a high level of insect resistance relative to close relatives with acylsugar profiles that not dominated by those with C7-C12 acyl groups (Thurston, 1961; Kroumova and Wagner, 2003). In *N. benthamiana*, the two most

abundant acylsugars that we found contain C7 and predominantly C8 acyl groups, which is consistent to previous findings of mainly 5- and 6-methyl heptanoate (C8) in *N. benthamiana* (Kroumova and Wagner, 2003; Slocombe et al., 2008) and in *N. alata* (Moghe et al., 2017). The almost complete depletion of acylsugars in our *ASAT2* mutants improved aphid and whitefly performance (Figure 4, 5A, S4, S6), suggesting that the identified C8-chain acyl group acylsugars are providing insect resistance for *N. benthamiana*. Increased water loss and leaf temperature in the *asat2-1* and *asat2-2* mutants (Figure 6, S7) is consistent with prior studies that suggested a role for acylsugars in tomato drought tolerance (Fobes et al., 1985; O' Connell et al., 2007; Kroumova et al., 2016).

The characterized acylsugars were reduced to a greater extent in *N. benthamiana ASAT2* than in *ASAT1* mutants (Figure 3). This observation has two implications. First, the reduction of acylsugars in *ASAT1* mutants indicates that *Nben*ASAT2 functions upstream of *Nben*ASAT1 in the acylsugar biosynthesis pathway. Second, the incomplete depletion of the acylsugars suggests that *Nben*ASAT1 functions may be partially compensated by other enzymes, perhaps including *Nben*ASAT2. In the ASAT phylogenetic tree (Figure 1), *Nben*ASAT2 is closely related to some biochemically characterized ASAT1 proteins in other Solanaceae species, including the *Spen*ASAT1, *Slyc*ASAT1, and *Snig*ASAT1. Those ASAT1s have some substrate overlap with the ASAT2s found in the corresponding species, indicating that ASAT2 has moved toward utilizing the ASAT1 substrate in these species over time (Moghe et al., 2017). The final activity shift that has become fixed in the *Solanum* genus most likely occurred after the divergence of the *Solanum* and *Capsicum* clades (Moghe et al., 2017). However, if our hypothesis of partial complementation of *Nben*ASAT1 by *Nben*ASAT2 is correct, it may flag a transition stage or suggest independent *Nicotiana*-specific evolution of the ASAT1/ASAT2 functions. Based on previous knowledge of BAHD activities (Moghe et al., 2017), we postulate that S2:15 (7,8) and S2:16 (8,8) are produced by NbenASAT1 and NbenASAT2, while the acetylation is carried out by another unrelated BAHD enzyme – not unlike the distantly related SlycASAT4 and *Salpiglossis sinuata* ASAT5 enzymes. Further characterization will be required to identify specific enzyme activities.

Although *ASAT1* mutations cause only a partial reduction in the acylsugar profile, they nevertheless lead to increased *M. persicae* size (Figure 4B, S4B). However, the absence of aphid preference for *ASAT1* mutants suggested that the insects were not able to detect the difference in the acylsugar content relative to wildtype *N. benthamiana.* Despite the only partial decrease in the acylsugar content of *ASAT1* mutants, the decreases in water content and increases in leaf temperature were similar to those of *ASAT2* mutants (Figure 6B, C, S7B, C). The water loss phenotypes of the *ASAT1* mutants likely resulted from the reduced abundance of acylsugars, as *asat1-1*, with a relatively higher reduction of acylsugars (Figure 3), has a lower leaf water content and a higher leaf temperature compared to those of

asat1-2 (Figure 6B, C, S7B, C). These results suggest that the two acylsucroses contribute to protecting *N. benthamiana* against drought.

Nicotiana benthamiana has been used for virus transmission assays, VIGS of *M. persicae* genes, and transient expression of genes from other species to determine their effects on aphid growth and reproduction (Del Toro et al.; Ramsey et al., 2007; Bos et al., 2010; Pitino and Hogenhout, 2013; Casteel et al., 2014; Elzinga et al., 2014; Rodriguez et al., 2014; Krenz et al., 2015; Tzin et al., 2015; Mulot et al., 2016; Mathers et al., 2017; Cui et al., 2019; Worrall et al., 2019). However, experiments of this kind are hampered by the fact that many *M. persicae* isolates do not perform well on *N. benthamiana*. Similarly, due to the very poor survival of *B. tabaci* on wildtype plants, *N. benthamiana* has not been useful as a host plant for whitefly research. Therefore, the availability of *N. benthamiana asat2* mutants will facilitate future research with both aphids and whiteflies.

Although both *H. virescens* and *T. ni* larvae grow well on cultivated tobacco, they did not survive or grew very slowly on both wildtype and *ASAT* mutant *N. benthamiana* (Figure 5B, C). This suggests that other resistance mechanisms in *N. benthamiana* provide protection against these lepidopteran species. Additional mutations that decrease insect resistance, perhaps regulatory genes such as *COI1* or genes affecting the production of specialized metabolites other than acylsugars, will be necessary to facilitate *N. benthamiana* experiments with these lepidopteran species.

Our knockout of acylsugar biosynthesis is an important first step toward developing the excellent *N. benthamiana* system as one that can also be used for studying plant interactions with *M. persicae*, *B. tabaci*, and perhaps other agriculturally relevant hemipteran pests. Such experiments can include transient expression assays to test the function of insect elicitors and insect-defensive genes from other plant species in *N. benthamiana*, as well as VIGS to down-regulate insect gene expression. Furthermore, the almost complete absence of acylsugars in the *ASAT2* mutant lines, in combination with the facile transient gene expression systems available for *N. benthamiana*, will make these mutants a suitable platform for the functional analysis of ASATs from other Solanaceae.

Materials and Methods

Insect and plant cultures

A red strain of *M. persicae* (Ramsey et al., 2007; Ramsey et al., 2014) originally collected from *N. tabacum* by Stewart Gray (Robert W. Holley Center for Agriculture & Health, Ithaca, NY) was maintained on *N. tabacum* plants in a growth room at 23°C with a 16:8 h light:dark photoperiod. Insect bioassays were conducted in the same growth room. Eggs of *H. virescens* and *T. ni* were purchased from Benzon Research (www.benzonresearch.com). *Nicotiana benthamiana* wild type and mutant plants for aphid and caterpillar experiments were maintained at 23°C and a 16:8 h light:dark photoperiod in a Conviron (Winnipeg, Canada) growth chamber and, for seed production, in a greenhouse at 27/24°C (day/night) with ambient light conditions. A virus-free *B. tabaci* MEAM1 colony was obtained from Jane E. Polston (University of Florida). *Nicotiana benthamiana* wild type and mutant plants for whitefly experiments were maintained at 26°C and a 16:8 h light:dark photoperiod in a growth room and, for seed production, in a growth chamber (Percival Scientific, Perry, IA) at 27/24°C (day/night) with a 16:8 h light:dark photoperiod.

Identification of ASAT1 and ASAT2 orthologs in N. benthamiana

To identify ASAT1 and ASAT2 orthologs in *N. benthamiana*, protein sequences of *Salpiglossis sinuate* and *Solanum lycopersicum* ASAT1 and ASAT2 (Moghe et al., 2017) were compared to predicted proteins encoded in the *N. benthamiana* genome. Sequences with >67% identity were selected as potential ASAT1 and ASAT2 candidates and nucleotide sequences were obtained from the Solanaceae Genomics Network (www.solgenomics.net). The candidate ASAT sequences also were confirmed by comparing them to the most recent published *N. benthamiana* genome assembly (Schiavinato et al., 2019). To confirm the nucleotide sequences of *N. benthamiana ASAT1* and *ASAT2*, genes were amplified with ASAT1F/ASAT1R and ASAT2F/ASAT2R primers (Table S2) using genomic DNA as the template. Amplified fragments were cloned in pDONOR™207 (ThermoFisher Scientific, US) and were sequenced in their entirety using Sanger sequencing. This confirmatory sequencing showed no differences relative to the published *N. benthamiana* genome.

Phylogenetic analysis of N. benthamiana ASATs

A protein phylogenetic tree of previously annotated Solanaceae ASATs (Figure 1, Figure S1; Table S1) was constructed using maximum likelihood method. Briefly, the ASATs protein sequences were aligned in program ClustalW (Thompson et al., 1994). Then the alignment was improved by removing the spurious sequences and poorly aligned regions (gap threshold at 0.25) in program TrimAL v 1.4.rev22 (Capella-Gutierrez et al., 2009). Finally, an unrooted maximum likelihood tree was generated using the

improved alignment with a bootstrap of 1000 in RAxML v8.2.12 (Stamatakis, 2014). The tree was visualized and presented using FigTree v1.4.4 (Computer program obtained from http://tree.bio.ed.ac.uk).

sgRNA design and plasmid cloning

Single-guide RNAs (sgRNA) targeting *ASAT1* and *ASAT2* were designed based on the coding regions using online software, CRISPR-P v2.0 (Liu et al., 2017) and CRISPRdirect (https://crispr.dbcls.jp/), based on two parameters, cleavage efficiency and potential off-targets. Additionally, only sgRNAs with >40% GC content were selected. Three Cas9/gRNA constructs each were constructed for *ASAT1* and *ASAT2* following a previously developed CRISPR/Cas9 system (Jacobs et al., 2015). Four segments of DNA were prepared with 20 bp overlaps on their ends: ssDNA gRNA oligo, linearized p201N:Cas9 plasmid (Addgene 59175-59178), the *Medicago truncatula* (Mt) U6 promoter (377bp), and a scaffold DNA (106bp). For ssDNA gRNA, oligos targeting either the sense or antisense of target genes were designed as: sense oligo TCAAGCGAACCAGTAGGCTT--GN_{19}--GTTTTAGAGCTAGAAATAGC, and antisense oligo GCTATTTCTAGCTCTAAAAC--N_{19}C—AAGCCTACTGGTTCGCTTGA. The gRNA oligo sequences were shown in (Figure 2 and Table S2). The oligo sequences were synthesized by Integrated DNA Technologies (www.idtdna.com), then 1 µl of each 100 µM oligo was added to 500 µl 1x NEB buffer 2 (New England Biolabs, www.neb.com). The p201N:Cas9 plasmid was linearized by digestion with *Spe*1 (www.neb.com) in 1x buffer 4 at 37°C for 2 h followed by a column purification and a second digestion with *Swa*I in 1 x buffer 3.1 at 25°C for 2 h. Complete digestions were confirmed on a 0.8% agarose gel. The MtU6 promoter and Scaffold DNAs were PCR-amplified from the pUC gRNA Shuttle plasmid (Jacobs et al., 2015) using the primers *Swa*I_MtU6F/MtU6R and ScaffoldF/Spe_ScaffoldR, respectively (Table S2). The PCR reactions were performed with a high-fidelity polymerase (2x Kapa master mix; www.sigmaaldrich.com) using the program: 95°C for 3 min followed by 31 cycles of 98°C for 20 sec, 60°C for 30 sec, 72°C for 30 sec, and a final extension of 72°C for 5 mins. Finally, cloning was done using the NEBuilder® HiFi DNA Assembly Cloning Kit. For each reaction, the four pieces of DNA were mixed in a 20 µl reaction with the NEBbuilder assembly mix with a final concentration of 0.011 pmol (~100 ng) of p201N:Cas9 plasmid, 0.2 pmol of MtU6 amplicon (~ 50 ng), scaffold amplicon (~ 12 ng) and ssDNA gRNA oligo (60-mer, 1 µl). The reactions were placed in thermal cycler at 50°C for 1 h. Then, 2 µl of the reaction were transformed into 50 µl of the One Shot™ Top10 chemically competent cells (Invitrogen, www.thermofisher.com) and plated with 50 µl/ml kanamycin selection. Colonies with correct inserts were screened using the primers of Ubi3p218R and IScelR (Table S2). Plasmids carrying the right gRNA constructs were then transformed into *Agrobacterium tumefaciens* strain GV3101 for generating transgenic plants. All constructs were confirmed by Sanger sequencing.

To avoid off-target effects, gRNAs were further checked by comparison against the reference *N. benthamiana* genome v1.0.1 (www.solgenomics.net). Only two sites were found to have non-target matches >17 nt (both with 1 internal mismatch), and with the NGG PAM sequence on the correct strand. These two sites were checked by PCR amplification and Sanger sequencing and showed no unexpected editing in our *asat1-1*, *asat1-2*, *asat2-1*, or *asat2-2* mutant plants. Primers used for off-target Sanger sequencing are listed in Table S2.

Transient mutagenesis of ASATs in N. benthamiana

For both *ASAT1* and *ASAT2*, we *Agrobacterium*-infiltrated *N. benthamiana* plants at the four-leaf stage. For *ASAT1*, we used *Agrobacterium* carrying the Cas9/gRNA constructs at OD of 1 and 3, whereas for *ASAT2*, we used an OD 1.5. Each leaf was saturated with *Agrobacterium* solution. After infiltration, the plants were cultured in a growth chamber for 2 days and then the infiltrated whole leaves were collected for genomic DNA extraction and tested by PCR amplification for detection of insertion/deletion polymorphisms in the target region (Figure S8). During the method optimization, a positive control construct targeting the *N. benthamiana Drm3* gene (gRNA: GCCACTATCTGGCCGGGGAC, provided by the Greg Martin lab, Boyce Thompson Institute) was infiltrated in parallel.

Stable mutagenesis of ASATs using tissue culture

The stable *ASAT* mutant *N. benthamiana* plants were created in the Boyce Thompson Institute plant transformation facility using CRISPR/Cas9 with gRNAs that had been confirmed to be functional as described above and a previously described protocol (Van Eck et al., 2019), with minor modifications. To prepare plants for transformation, we disinfected *N. benthamiana* seeds with 1.5 ml 1.25% sodium hypochlorite (1:5 dilution of 5.25% sodium hypochlorite Clorox bleach), with 100 µl Tween-20 added, for 20 min on a shaker platform. After sodium hypochlorite treatment, seeds were rinsed three times with sterile water. Subsequently, we placed seeds on Tobacco Seed Germination Medium (composition per liter: 1.08g Murashige and Skoog salt formulation, 30g sucrose, and 8 g agar, pH=5.7±0.1) and incubated the seeds under yellow filtered light with a 16-hr photoperiod at 27°C. After ~2 weeks, the seedlings were transferred to the Rooting Medium (composition per liter: 2.15 g Murashige and Skoog salt formulation, 30 g sucrose, 1 ml B5 vitamin/amino acid stock, and 8 g agar, pH=5.7±0.1). After ~6 weeks, the plants were ready for *Agrobacterium* infection. First, *Agrobacterium* carrying the gRNA plasmids was amplified in YEP medium (composition per liter: 10g yeast extract, 10g peptone, and 5g NaCl with antibiotics, 50 µg/µl gentamycin, 50 µg/µl kanamycin, and 50 µg/µl rifampicin), and *Agrobacterium* culture then was pelleted and combined to a certain OD (OD 1.0 for *ASAT1* gRNAs, and OD 1.0 or 1.5 for *ASAT2* gRNAs) with filtered cell suspension buffer (10 mM MES, 10 mM $MgCl_2$ and 200 µM acetosyringone). Then,

fully expanded but immature *N. benthamiana* leaves were dissected into 5 mm segments by removing the leaf margins. The leaf segments were incubated in the *Agrobacterium* culture for 30 min with shaking. The incubated leaf segments were transferred to co-cultivation medium plates (composition per liter: 4.3g Murashige and Skoog salt formulation, 30g sucrose, 1 ml B5 vitamin/amino acid stock, and 5g agar, pH=5.7±0.1) and kept in the dark at room temperature. Leaf segments treated with YEP medium were used as a negative control. After three days, the leaf segments were transferred from co-cultivation medium to shoot bud initiation medium with selections (composition per liter: 4.3g Murashige and Skoog salt formulation, 30g sucrose, 1 ml B5 vitamin/amino acid stock, 0.1 mg NAA, 1.0 mg BA, and 6g agar, pH=5.7±0.1; with 200 μg/ml kanamycin and 250 μg/ml Timentin). Medium with Timentin but without kanamycin was used as a positive control. Leaf segments on selection medium were incubated under a 16:8 h light-dark photoperiod at 24-25°C under yellow filtered light. The leaf segments were sub-cultured every 2-weeks onto the same medium until shoot buds were visible. Finally, to generate roots, shoot buds were transferred to rooting medium (composition per liter: 2.15g Murashige and Skoog salt formulation, 30g sucrose, 1 ml B5 vitamin/amino acid stock, 8g agar with 200 μg/ml kanamycin and 250 μg/ml Timentin, pH=5.7±0.1).

Rooted plants from tissue culture were transferred to soil and checked for the intended mutations by PCR amplification and Sanger sequencing. Confirmed homozygous *ASAT1* and *ASAT2* mutants were kept for seed collection. The presence of gRNA and Cas9 in transgenic plants also was confirmed using PCR (MtU6252F/p201R primer pair for gRNAs, and Cas9F7/nosT-rev2 primer pair for Cas9) (Table S2).

Acylsugar measurements by LC/MS

Liquid chromatography/mass spectrometry (LC/MS) was used to confirm the effect of the *ASAT* mutations by measuring acylsugar content in leaf extracts from wildtype and *ASAT* mutant plants. New leaflets were rinsed in acylsugar extraction solution (3:3:2 acetonitrile:isopropanol:water, 0.1% formic acid, and 1 μM Telmisartan as internal standard) and gently agitated for 2 min. Then, the extraction solutions were transferred to LC/MS glass vials, and the leaves were air dried for leaf weight measurements.

Chromatography of leaf surface washes was performed on a ThermoScientific Ultimate 3000 HPLC with a glass vial autosampler and coupled with a Thermo Scientific Q Exactive™ Hybrid Quadrupole-Orbitrap™ Mass Spectrometer (Mass Spectrometry Facility at Boyce Thompson Institute). Acylsugar extracts were separated on an Ascentis Express C18 HPLC column (10 cm × 2.1 mm × 2.7 μm) (Sigma-Aldrich, St. Louis, MO) with a flow rate of 0.3 ml/min, using a gradient flow of 0.1% formic acid (Solvent A) and 100% acetonitrile (Solvent B). We used a 7-min LC method for metabolite profiling involved a linear gradient from 95:5 A:B to 0:98 A:B. Full-scan mass spectra were collected (mass range:

m/z 50–1000) in both positive and negative electron spray ionization (ESI) modes. Mass spectral parameters were set as follows: capillary spray voltage 2.00 kV for negative ion-mode and 3.00 kV for positive ion-mode, Source temperature: 100°C, desolvation temperature 350°C, desolvation nitrogen gas flow rate: 600 liters/h, cone voltage 35 V. Acylsugars were identified and annotated using Thermo Xcalibur Qual Browser (Thermo Fisher) and MS-DIAL v4.20 based on the MS/MS peak features and neutral losses. The acylsugar abundances were estimated using peak areas at the respective *m/z* channel under negative ESI mode. Acylsugar quantification was first normalized to the internal control Telmisartan to account for technical variation between samples, and then normalized to the leaf dry weight to allow comparisons between samples.

Insect bioassays

To measure aphid growth on *ASAT* mutant and wildtype plants, we placed two leaf cages on each plant (Figure S9A). Twenty adult aphids from *N. tabacum* (naïve to *N. benthamiana*) were placed in each cage and allowed to generate nymphs for ~12 hrs. Twenty-five nymphs were left in each cage and were monitored for 120 hours to assess nymph survival. At the end of aphid survival monitoring period, five aphids were left in each cage and reproduction was monitored for one week. Finally, the remaining aphids were collected to measure aphid size by taking a picture and assessing the area of each aphid using ImageJ (Schneider et al., 2012).

Aphids choice assays were performed with detached leaves. Briefly, similarly-sized leaves from eight individual *ASAT* mutant and wildtype plants were cut and placed at each side of 15-cm Petri dishes, with their petioles inserted in moistened cotton swabs (Figure S9B). Ten naïve adult aphids, which had not previously encountered *N. benthamiana*, were released at the midpoint in between wildtype and *asat1* or *asat2* leaves, and the Petri dishes were placed in complete darkness. The aphids on each leaf were counted at 24 h after their release in the Petri dishes.

To measure whitefly survival and fecundity on wildtype and *ASAT2* mutant *N. benthamiana* plants, we placed three plants at the seven-leaf stage in each of two cages. Ninety adult whiteflies reared on *Brassica oleracea* (cabbage variety Earliana; Burpee catalog number 62729A) were introduced into each cage with *N. benthamiana* (30 whiteflies/plant) and were allowed to feed for three days. The numbers of whiteflies surviving on each host plant were counted, after which the remaining insects were terminated using insecticidal soap. The following day, the number of whitefly eggs on each plant were counted.

Eggs of *H. virescens* and *T. ni* were hatched on artificial diet (Southland Products, Lake Village, Arkansas). Neonate larvae were confined onto individual *N. benthamiana* leaves, one larva per plant, using organza mesh bags. After ten days, the surviving larvae were counted and weighed.

Leaf desiccation assay

To measure the leaf water loss, two leaves from each of eight plants were detached. The fresh weight of each leaf was determined on a Sartorius Ultra Micro Balance. All leaves were placed at 23°C and a 16:8 h light:dark photoperiod. Each leaf was weighted after 24 hours and the percentage of water loss was calculated as [-(final weight - fresh weight)/fresh weight]*100%.

Thermal and hyperspectral imaging

Thermal images were acquired in the growth chamber environment using a thermal camera (A655sc, FLIR Systems Inc., Boston, MA, USA) with a spectral range of 7.5–14.0 mm and a resolution of 640 x 480 pixels. The camera was placed approximately 1 m away from each plant and a white background was used when the plant images were acquired. One region of interest, corresponding to the perimeter of each leaf, was specified per leaf for each of 20 leaves per genotype. Using the FLIR ResearchIR Max software (version 4.40.9.30) thermal images files were exported as CSV files. Images were segmented from the background using Gaussian mixture models in MATLAB to determine the temperature of each leaf. After segmentation, the temperature was averaged across the segmented leaf.

Hyperspectral images were acquired in a dark room using a hyperspectral imager (SOC710, Series 70-V, Surface Optics Corporation, San Diego, CA, USA) that covered a spectral range from 400 to 1000 nm for 128 wavebands. Image acquisition and recording were performed using a Dell DELL XPS 15 9570 laptop computer that controls the camera. The camera was fixed using a stand with the lens facing the plants and capturing top view images approximately 1 m away. A Spectralon tile (Labsphere, Inc, North Sutton NH, USA) was placed next to the plant trays, covering one corner of the image to facilitate subsequent image processing and calibration. The nominal reflectance value for the Spectralon tile was 99% and it had a 30.5cm x 30.5cm reflective area. Lighting consisted of two halogen lamps placed at ~ 45° angles on either side of the camera to create an even light distribution. All image analysis was performed in HSIviewer, a MATLAB package (Stone et al., 2020). White reflectance calibration was performed using the Spectralon tile. One region of interest ROI was specified for each of 20 leaves per *N. benthamiana* genotype. This ROI corresponded to the perimeter of each leaf. From each hyperspectral cube image, the vegetation pixels (green portion of the plant) were extracted using the Normalized Difference Vegetation Index (NDVI). Mean reflectance (R) was calculated per band per 10 leaves in order to obtained the WBI results

To calculate NDVI and WBI we used the following formulas, where *R* corresponds to the reflectance at a specific wavelength (nm): WBI = (R970/R900) (Penuelas et al., 1993) and NVDI = (R750 - R705)/(R750 + R705) (Gitelson and Merzlyak, 1994).

Statistical analysis

All statistical comparisons were conducted using SPSS v25, R and MATLAB R2019a (MathWorks, Inc., Natick, MA, USA). ANOVA followed by a Dunnett's post hoc test was used to determine differences in leaf water loss, leaf temperature, and WBI across genotypes in each data set. ANOVA followed by a Duncan post hoc test was used for aphid bioassay and LC/MS results. A two-tailed independent samples *t*-test was used to test for differences in pairwise aphid-choice assays, whitefly, and lepidopteran assays.

Acknowledgements

We want to thank Patricia Keen and Joyce Van Eck for their help with *N. benthamiana* stable transformation and access to the tissue culture facility, Ning Zhang and Greg Martin for sharing the p201N-Cas9 construct and the *Drm3* sgRNA control construct, and William Stone and Thomas Lawton for providing custom image processing software. This research was supported by Cornell startup funds to G.D.M., Deutsche Forschungsgemeinschaft award #411255989 to L.H.K., and United States Department of Agriculture Biotechnology Risk Assessment Grant 2017-33522-27006, US National Science Foundation award IOS-1645256, and Defense Advanced Research Projects Agency (DARPA) agreement HR0011-17-2-0053 to G.J. G.S. is part of a team supporting DARPA's Insect Allies program under agreement HR0011-17-2-0055. M.A.G. is part of a team supporting DARPA's Advanced Plant Technologies program under agreement HR0011-18-C-0146. The views and conclusions contained in this document are those of the authors and should not be interpreted as representing the official policies of the U.S. Government.

Conflict of interest

The authors declare that there is no conflict of interest.

Author Contributions

G.J. and H.F. conceived the original research plans; H.F., S.S., L.A., H.X., L.K. and A. N. F. performed the experiments; H.F., L.A., L.K., and G.D.M. analyzed the data; M.A.G., G.D.M., G.S. and G.J. supervised the experiments; H.F. and G.J. wrote the article with contributions of all the authors; G.J. agrees to serve as the contact author responsible for communication and distribution of samples.

References

Alba JM, Montserrat M, Fernandez-Munoz R (2009) Resistance to the two-spotted spider mite (*Tetranychus urticae*) by acylsucroses of wild tomato (*Solanum pimpinellifolium*) trichomes studied in a recombinant inbred line population. Experimental and Applied Acarology **47:** 35-47

Arntzen C (2015) Plant-made pharmaceuticals: from 'Edible Vaccines' to Ebola therapeutics. Plant Biotechnology Journal **13:** 1013-1016

Arrendale RF, Severson RF, Sisson VA, Costello CE, Leary JA, Himmelsbach DS, Vanhalbeek H (1990) Characterization of the sucrose ester fraction from *Nicotiana glutinosa*. Journal of Agricultural and Food Chemistry **38:** 75-85

Bally J, Jung H, Mortimer C, Naim F, Philips JG, Hellens R, Bombarely A, Goodin MM, Waterhouse PM (2018) The rise and rise of *Nicotiana benthamiana*: a plant for all reasons. Annual Review of Phytopathology, Vol 56 **56:** 405-426

Bombarely A, Rosli HG, Vrebalov J, Moffett P, Mueller LA, Martin GB (2012) A draft genome sequence of *Nicotiana benthamiana* to enhance molecular plant-microbe biology research. Mol Plant-Micr Int **25:** 1523-1530

Bos JIB, Prince D, Pitino M, Maffei ME, Win J, Hogenhout SA (2010) A functional genomics approach identifies candidate effectors from the aphid species *Myzus persicae* (green peach aphid). Plos Genetics **6:** e1001216.

Capella-Gutierrez S, Silla-Martinez JM, Gabaldon T (2009) trimAl: a tool for automated alignment trimming in large-scale phylogenetic analyses. Bioinformatics **25:** 1972-1973

Cardoso MZ (2008) Herbivore handling of a plant's trichome: The case of *Heliconius charithonia* (L.) (Lepidoptera : Nymphalidae) and *Passiflora Lobata* (Killip) Hutch. (Passifloraceae). Neotropical Entomology **37:** 247-252

Casteel CL, Yang CL, Nanduri AC, De Jong HN, Whitham SA, Jander G (2014) The NIa-Pro protein of *Turnip mosaic virus* improves growth and reproduction of the aphid vector, *Myzus persicae* (green peach aphid). Plant Journal **77:** 653-663

Chortyk OT, Pomonis JG, Johnson AW (1996) Syntheses and characterizations of insecticidal sucrose esters. Journal of Agricultural and Food Chemistry **44:** 1551-1557

Cui N, Lu H, Wang TZ, Zhang WH, Kang L, Cui F (2019) Armet, an aphid effector protein, induces pathogen resistance in plants by promoting the accumulation of salicylic acid. Philosophical Transactions of the Royal Society B-Biological Sciences **374**

Del Toro FJ, Mencía E, Aguilar E, Tenllado F, Canto T HCPro-mediated transmission by aphids of purified virions does not require its silencing suppression function and correlates with its ability to coat cell microtubules in loss-of-function mutant studies. Virology **525:** 10-18

Egan AN, Moore S, Stellari GM, Kang BC, Jahn MM (2019) Tandem gene duplication and recombination at the AT3 locus in the *Solanaceae*, a gene essential for capsaicinoid biosynthesis in *Capsicum*. Plos One **14:** e0210510

Egea I, Albaladejo I, Meco V, Morales B, Sevilla A, Bolarin MC, Flores FB (2018) The drought-tolerant *Solanum pennellii* regulates leaf water loss and induces genes involved in amino acid and ethylene/jasmonate metabolism under dehydration. Sci Rep **8:** 2791

Ellison EE, Nagalakshmi U, Gamo ME, Huang PJ, Dinesh-Kumar S, Voytas DF (2020) Multiplexed heritable gene editing using RNA viruses and mobile single guide RNAs. Nat Plants **6:** 620-624

Elzinga DA, De Vos M, Jander G (2014) Suppression of plant defenses by a *Myzus persicae* (green peach aphid) salivary effector protein. Mol Plant Microbe Interact **27:** 747-756

Fan P, Miller AM, Schilmiller AL, Liu X, Ofner I, Jones AD, Zamir D, Last RL (2016) In vitro reconstruction and analysis of evolutionary variation of the tomato acylsucrose metabolic network. Proc Natl Acad Sci U S A **113:** E239-248

Fobes JF, Mudd JB, Marsden MP (1985) Epicuticular lipid accumulation on the leaves of *Lycopersicon pennellii* (Corr.) D'Arcy and *Lycopersicon esculentum* Mill. Plant Physiol **77:** 567-570

Gaquerel E, Kotkar H, Onkokesung N, Galis I, Baldwin IT (2013) Silencing an N-acyltransferase-like involved in lignin biosynthesis in *Nicotiana attenuata* dramatically alters herbivory-induced phenolamide metabolism. Plos One **8:** e62336

Gitelson A, Merzlyak MN (1994) Spectral reflectance changes associated with autumn senescence of *Aesculus hippocastanum* L and *Acer platanoides* L leaves - spectral features and relation to chlorophyll estimation. J Plant Physiol **143:** 286-292

Glas JJ, Schimmel BCJ, Alba JM, Escobar-Bravo R, Schuurink RC, Kant MR (2012) Plant glandular trichomes as targets for breeding or engineering of resistance to herbivores. International Journal of Molecular Sciences **13:** 17077-17103

Gong P, Zhang J, Li H, Yang C, Zhang C, Zhang X, Khurram Z, Zhang Y, Wang T, Fei Z, Ye Z (2010) Transcriptional profiles of drought-responsive genes in modulating transcription signal transduction, and biochemical pathways in tomato. J Exp Bot **61:** 3563-3575

Goodin MM, Zaitlin D, Naidu RA, Lommel SA (2008) *Nicotiana benthamiana*: its history and future as a model for plant-pathogen interactions. Mol Plant Microbe Interact **21:** 1015-1026

Hagimori M, Matsui M, Matsuzaki T, Shinozaki Y, Shinoda T, Harada H (1993) Production of somatic hybrids between *Nicotiana benthamiana* and *Nicotiana tabacum* and their resistance to aphids. Plant Science **91:** 213-222

Hayward A, Padmanabhan M, Dinesh-Kumar SP (2011) Virus-induced gene silencing in *Nicotiana benthamiana* and other plant species. Plant Reverse Genetics: Methods and Protocols **678:** 55-63

Jacobs TB, LaFayette PR, Schmitz RJ, Parrott WA (2015) Targeted genome modifications in soybean with CRISPR/Cas9. Bmc Biotechnology **15:** 16

Kandra L, Wagner GJ (1988) Studies of the site and mode of biosynthesis of tobacco trichome exudate components. Archives of Biochemistry and Biophysics **265:** 425-432

Karabourniotis G, Kotsabassidis D, Manetas Y (1995) Trichome density and its protective potential against ultraviolet-B radiation damage during leaf development. Canadian Journal of Botany-Revue Canadienne De Botanique **73:** 376-383

Kim J, Kang K, Gonzales-Vigil E, Shi F, Jones AD, Barry CS, Last RL (2012) Striking natural diversity in glandular trichome acylsugar composition is shaped by variation at the acyltransferase2 locus in the wild tomato *Solanum habrochaites*. Plant Physiol **160:** 1854-1870

Krenz B, Bronikowski A, Lu XY, Ziebell H, Thompson JR, Perry KL (2015) Visual monitoring of *Cucumber mosaic virus* infection in *Nicotiana benthamiana* following transmission by the aphid vector *Myzus persicae*. Journal of General Virology **96:** 2904-2912

Kroumova AB, Wagner GJ (2003) Different elongation pathways in the biosynthesis of acyl groups of trichome exudate sugar esters from various solanaceous plants. Planta **216:** 1013-1021

Kroumova ABM, Zaitlin D, Wagner GJ (2016) Natural variability in acyl moieties of sugar esters produced by certain tobacco and other *Solanaceae* species. Phytochemistry **130:** 218-227

Laue G, Preston CA, Baldwin IT (2000) Fast track to the trichome: induction of N-acyl nornicotines precedes nicotine induction in *Nicotiana repanda*. Planta **210:** 510-514

Leong BJ, Lybrand DB, Lou YR, Fan PX, Schilmiller AL, Last RL (2019) Evolution of metabolic novelty: A trichome-expressed invertase creates specialized metabolic diversity in wild tomato. Science Advances **5:** eaaw3754

Liu H, Ding YD, Zhou YQ, Jin WQ, Xie KB, Chen LL (2017) CRISPR-P 2.0: an improved CRISPR-Cas9 tool for genome editing in plants. Molecular Plant **10:** 530-532

Mathers TC, Chen Y, Kaithakottil G, Legeai F, Mugford ST, Baa-Puyoulet P, Bretaudeau A, Clavijo B, Colella S, Collin O, Dalmay T, Derrien T, Feng H, Gabaldon T, Jordan A, Julca I, Kettles GJ, Kowitwanich K, Lavenier D, Lenzi P, Lopez-Gomollon S, Loska D, Mapleson D, Maumus F, Moxon S, Price DR, Sugio A, van Munster M, Uzest M, Waite D, Jander G, Tagu D, Wilson ACC, van Oosterhout C, Swarbreck D, Hogenhout SA (2017) Rapid transcriptional plasticity of duplicated gene clusters enables a clonally reproducing aphid to colonise diverse plant species. Genome Biology **18:** 27

Matsuzaki T, Shinozaki Y, Hagimori M, Tobita T, Shigematsu H, Koiwai A (1992) Novel glycerolipids and glycolipids from the surface-lipids of *Nicotiana benthamiana*. Bioscience Biotechnology and Biochemistry **56:** 1565-1569

Matsuzaki T, Shinozaki Y, Suhara S, Ninomiya M, Shigematsu H, Koiwai A (1989) Isolation of glycolipids from the surface-lipids of *Nicotiana bigelovii* and their distribution in *Nicotiana* species. Agricultural and Biological Chemistry **53:** 3079-3082

McKenzie CL, Puterka GJ (2004) Effect of sucrose octanoate on survival of nymphal and adult *Diaphorina citri* (Homoptera : Psyllidae). Journal of Economic Entomology **97:** 970-975

Moghe GD, Leong BJ, Hurney SM, Jones AD, Last RL (2017) Evolutionary routes to biochemical innovation revealed by integrative analysis of a plant-defense related specialized metabolic pathway. Elife **6:** e28468

Mulot M, Boissinot S, Monsion B, Rastegar M, Clavijo G, Halter D, Bochet N, Erdinger M, Brault V (2016) Comparative analysis of RNAi-based methods to down-regulate expression of two genes expressed at different levels in *Myzus persicae*. Viruses **8:** 316

Ning J, Moghe GD, Leong B, Kim J, Ofner I, Wang Z, Adams C, Jones AD, Zamir D, Last RL (2015) A feedback-insensitive isopropylmalate synthase affects acylsugar composition in cultivated and wild tomato. Plant Physiol **169:** 1821-1835

O' Connell MA, Medina AL, Sanchez Pena Pand Trevino MB (2007) Molecular genetics of drought resistance response in tomato and related species. In Razdan, M. K., & Mattoo, A. K. (eds). Genetic Improvement of Solanaceous Crops **2:** Enfield USA 261-283

Penuelas J, Filella I, Biel C, Serrano L, Save R (1993) The reflectance at the 950-970 nm region as an indicator of plant water status. International Journal of Remote Sensing **14:** 1887-1905

Pitino M, Hogenhout SA (2013) Aphid protein effectors promote aphid colonization in a plant species-specific manner. Molecular Plant-Microbe Interactions **26:** 130-139

Powell JD (2015) From pandemic preparedness to biofuel production: tobacco finds its biotechnology niche in North America. Agriculture-Basel **5:** 901-917

Ramsey JS, Elzinga DA, Sarkar P, Xin YR, Ghanim M, Jander G (2014) Adaptation to nicotine feeding in *Myzus persicae*. J Chem Ecol **40:** 869-877

Ramsey JS, Wilson AC, de Vos M, Sun Q, Tamborindeguy C, Winfield A, Malloch G, Smith DM, Fenton B, Gray SM, Jander G (2007) Genomic resources for *Myzus persicae*: EST sequencing, SNP identification, and microarray design. BMC Genomics **8:** 423

Rodriguez AE, Tingey WM, Mutschler MA (1993) Acylsugars of *Lycopersicon pennellii* deter settling and feeding of the green peach aphid (Homoptera, Aphididae). Journal of Economic Entomology **86:** 34-39

Rodriguez PA, Stam R, Warbroek T, Bos JIB (2014) Mp10 and Mp42 from the aphid species *Myzus persicae* trigger plant defenses in *Nicotiana benthamiana* through different activities. Molecular Plant-Microbe Interactions **27:** 30-39

Schiavinato M, Strasser R, Mach L, Dohm JC, Himmelbauer H (2019) Genome and transcriptome characterization of the glycoengineered *Nicotiana benthamiana* line DeltaXT/FT. BMC Genomics **20:** 594

Schilmiller A, Shi F, Kim J, Charbonneau AL, Holmes D, Jones AD, Last RL (2010) Mass spectrometry screening reveals widespread diversity in trichome specialized metabolites of tomato chromosomal substitution lines. Plant Journal **62:** 391-403

Schilmiller AL, Charbonneau AL, Last RL (2012) Identification of a BAHD acetyltransferase that produces protective acyl sugars in tomato trichomes. Proc Natl Acad Sci U S A **109:** 16377-16382

Schneider CA, Rasband WS, Eliceiri KW (2012) NIH Image to ImageJ: 25 years of image analysis. Nature Methods **9:** 671-675

Shepherd RW, Wagner GJ (2007) Phylloplane proteins: emerging defenses at the aerial frontline? Trends in Plant Science **12:** 51-56

Simmons AT, Gurr GM, McGrath D, Martin PM, Nicol HI (2004) Entrapment of *Helicoverpa armigera* (Hubner) (Lepidoptera:Noctuidae) on glandular trichomes of *Lycopersicon* species. Australian Journal of Entomology **43:** 196-200

Simon B, Cenis JL, Demichelis S, Rapisarda C, Caciagli P, Bosco D (2003) Survey of *Bemisia tabaci* (Hemiptera: Aleyrodidae) biotypes in Italy with the description of a new biotype (T) from *Euphorbia characias*. Bull Entomol Res **93:** 259-264

Slocombe SP, Schauvinhold I, McQuinn RP, Besser K, Welsby NA, Harper A, Aziz N, Li Y, Larson TR, Giovannoni J, Dixon RA, Broun P (2008) Transcriptomic and reverse genetic analyses of branched-chain fatty acid and acyl sugar production in *Solanum pennellii* and *Nicotiana benthamiana*. Plant Physiol **148:** 1830-1846

Song Z, Li S, Chen X, Liu L, Z S (2006) Synthesis of insecticidal sucrose esters. Forestry Studies in China **8:** 26-29

Stamatakis A (2014) RAxML version 8: a tool for phylogenetic analysis and post-analysis of large phylogenies. Bioinformatics **30:** 1312-1313

Stone WD, Pellicore MJ, Hagstrom S, Lawton TJ (2020) HSIviewer: Pushbutton hyperspectral image analysis for rapid plant phenotyping. in review

Thompson JD, Higgins DG, Gibson TJ (1994) Clustal-W - Improving the sensitivity of progressive multiple sequence alignment through sequence weighting, position-specific gap penalties and weight matrix choice. Nucleic Acids Research **22:** 4673-4680

Thurston R (1961) Resistance in *Nicotiana* to the green peach aphids and some other tobacco insect pest. Journal of Economic Entomology **54:** 946-949

Tzin V, Yang X, Jing X, Zhang K, Jander G, Douglas AE (2015) RNA interference against gut osmoregulatory genes in phloem-feeding insects. J Insect Physiol **79:** 105-112

Van Eck J, Keen P, Tjahjadi M (2019) *Agrobacterium tumefaciens*-mediated transformation of tomato. Methods Mol Biol **1864:** 225-234

Van T, Weinhold A, Ullah C, Dressel S, Schoettner M, Gase K, Gaquerel E, Xu SQ, Baldwin IT (2017) O-acyl sugars protect a wild tobacco from both native fungal pathogens and a specialist herbivore. Plant Physiology **174:** 370-386

Wagner GJ, Wang E, Shepherd RW (2004) New approaches for studying and exploiting an old protuberance, the plant trichome. Annals of Botany **93:** 3-11

Weinhold A, Baldwin IT (2011) Trichome-derived O-acyl sugars are a first meal for caterpillars that tags them for predation. Proceedings of the National Academy of Sciences of the United States of America **108:** 7855-7859

Worrall EA, Bravo-Cazar A, Nilon AT, Fletcher SJ, Robinson KE, Carr JP, Mitter N (2019) Exogenous application of RNAii-inducing double-stranded rna inhibits aphid-mediated transmission of a plant virus. Front Plant Sci **10:** 265

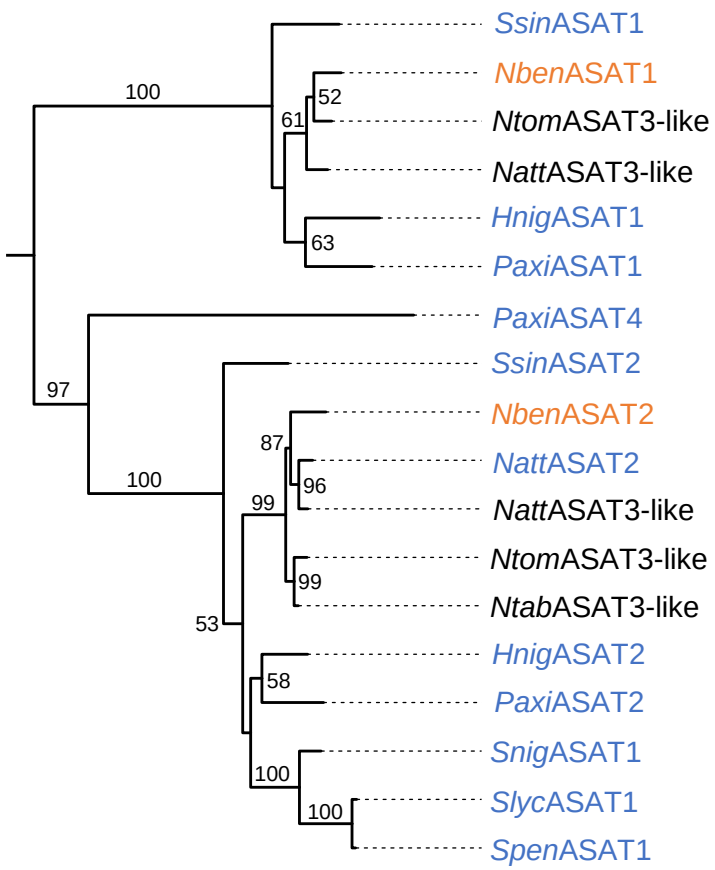

Figure 1. ASAT phylogenetic tree

The evolutionary history of ASATs in the Solanaceae (Table S1) was inferred using the Maximum Likelihood method using RAxML. Presented is a subtree of a larger tree that includes all annotated ASATs (Figure S1). The branch labels indicate the percentage of trees in which the associated taxa clustered together (bootstrap of 1000). Only values greater than 50 are presented. The two predicted *N. benthamiana* ASATs are highlighted in orange and ASATs that were previously chemically characterized are highlighted in blue.

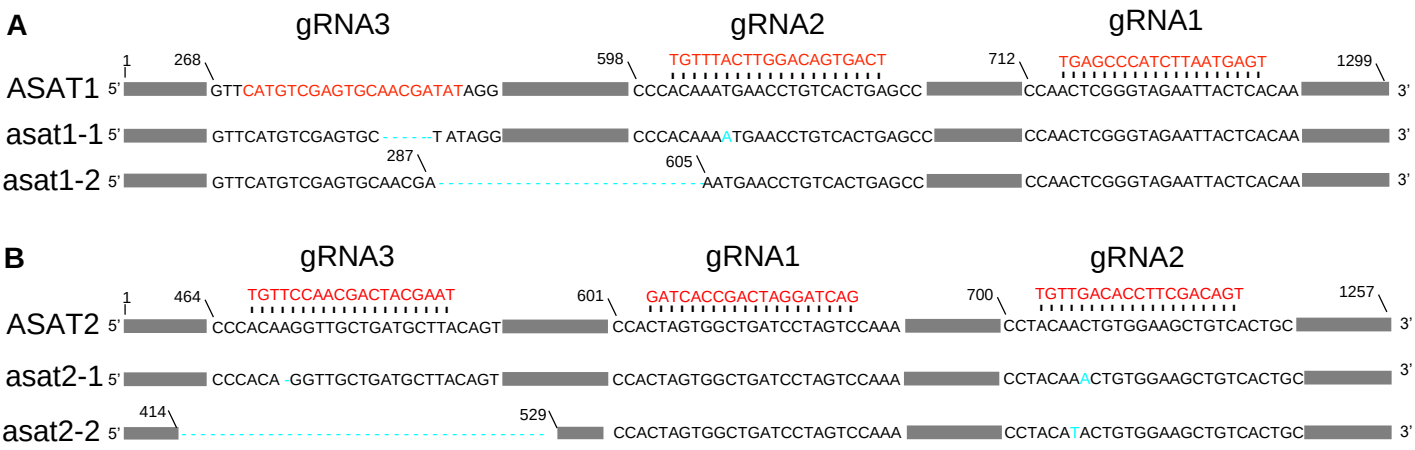

Figure 2. *N. benthamiana ASAT* mutations produced with CRISPR/Cas9
Three gRNAs (sequences shown in red) were designed to edit either *ASAT1* or *ASAT2*. For both *ASAT1* and *ASAT2*, we obtained two distinct mutations resulting from the corresponding gRNA2 and gRNA3. Single-base mutations and deletions are shown in cyan. **A**) *asat1-1* has a five-nucleotide deletion at gRNA3 and a single-nucleotide insertion at gRNA2. *asat1-2* has a 318-nucleotide deletion between the gRNA3 and gRNA2 cutting sites. **B**) *asat2-1* has a single nucleotide deletion at gRNA3 and single nucleotide insertion at gRNA2 leading to a translation frame shift between the two mutations. *asat2-2* has a 115-nucleotide deletion at gRNA3 and a single-nucleotide insertion leading to a translation frame shift at gRNA2.

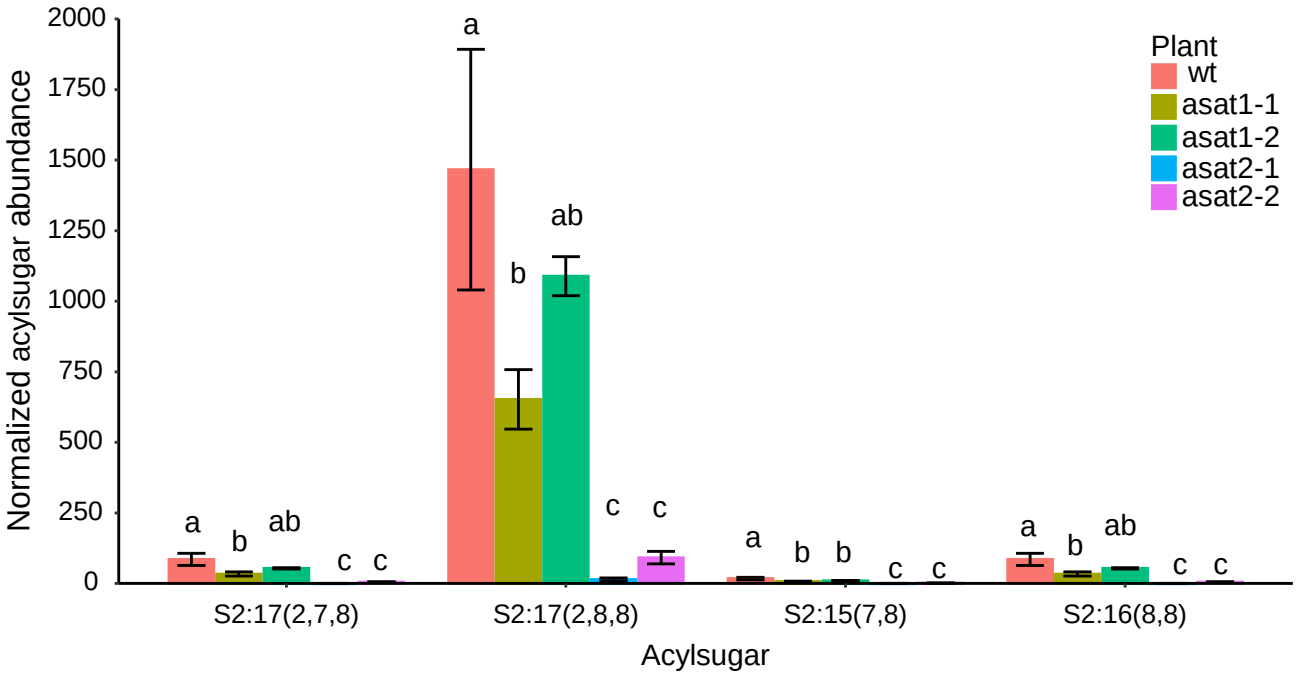

Figure 3. The abundances of two *N. benthamiana* acylsugars (S2:17(2,7,8) and S2:18(2,8,8)), and two likely pathway intermediates/fragmentations (S2:15(7,8) and S2:16(8,8))

Acyl sugar LC/MS peak areas were normalized relative to the peak area of Telmisartan, which was added as an internal control, and then to the leaf dry weight (per gram). Error bars represent standard errors from measurements of three plants of each genotype. Significant differences for each acylsugar between different genotypes were tested using one-way ANOVA followed by a Duncan's post hoc test ($p < 0.05$). Differences between groups are denoted with letters.

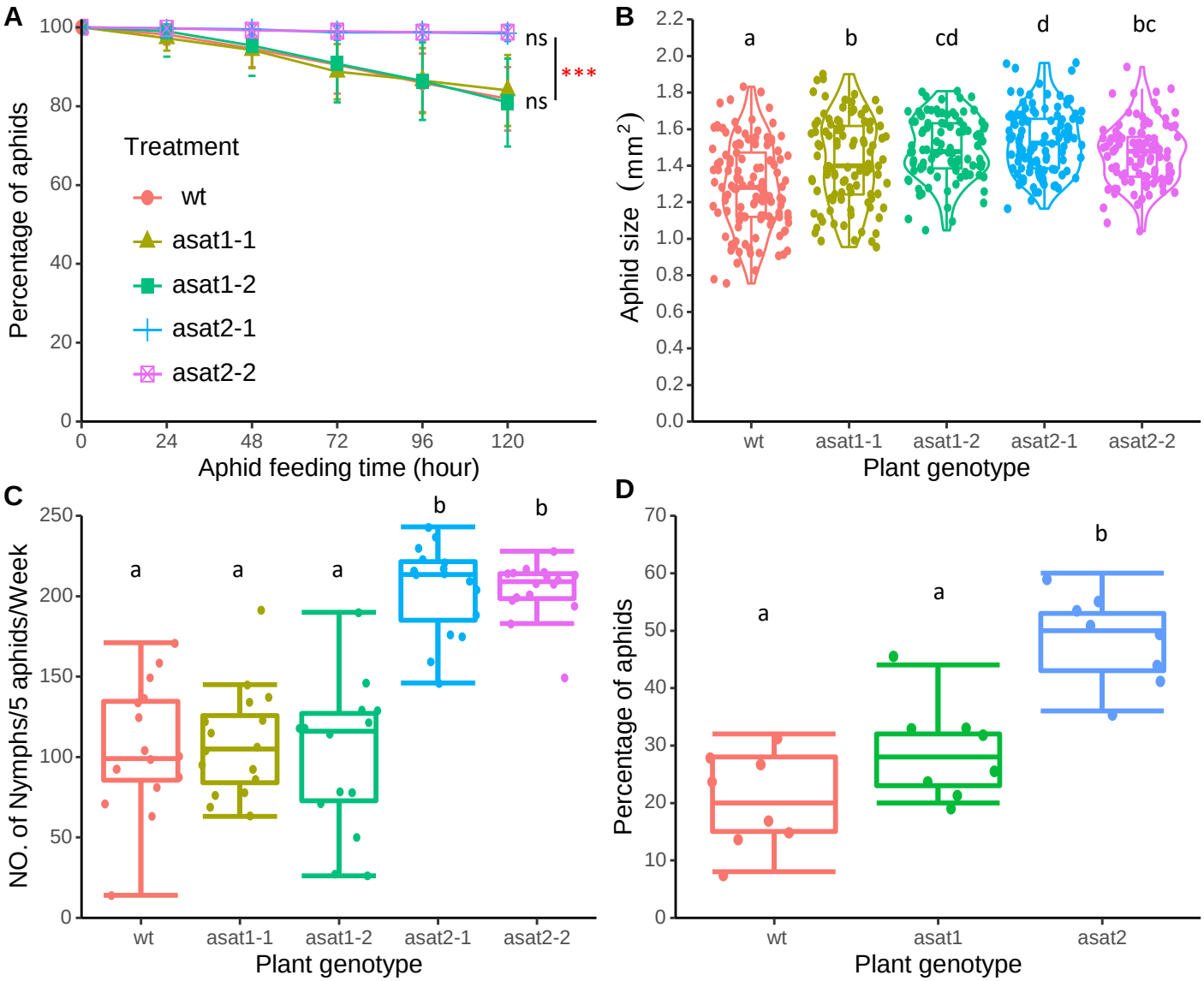

Figure 4. ***Myzus persicae*** **bioassays with wildtype,** ***asat1*****, and** ***asat2 N. benthamiana***
(A) Aphid survivorship over five days, ns: not significant, *** $p < 0.001$, *t*-test. **(B)** Aphid growth, as measured by = body sizes after 120 hours feeding on *N. benthamiana*. **(C)** Aphid reproduction, as measured by the number of nymphs that were reproduced by five aphids in one week. **(D)** Aphid choice among detached leaves of each plant genotype. Significant differences between different groups ($p < 0.05$) were determined using ANOVA followed by a Duncan's post hoc test and are indicated by lowercase letters above each group in panels B, C, and D.

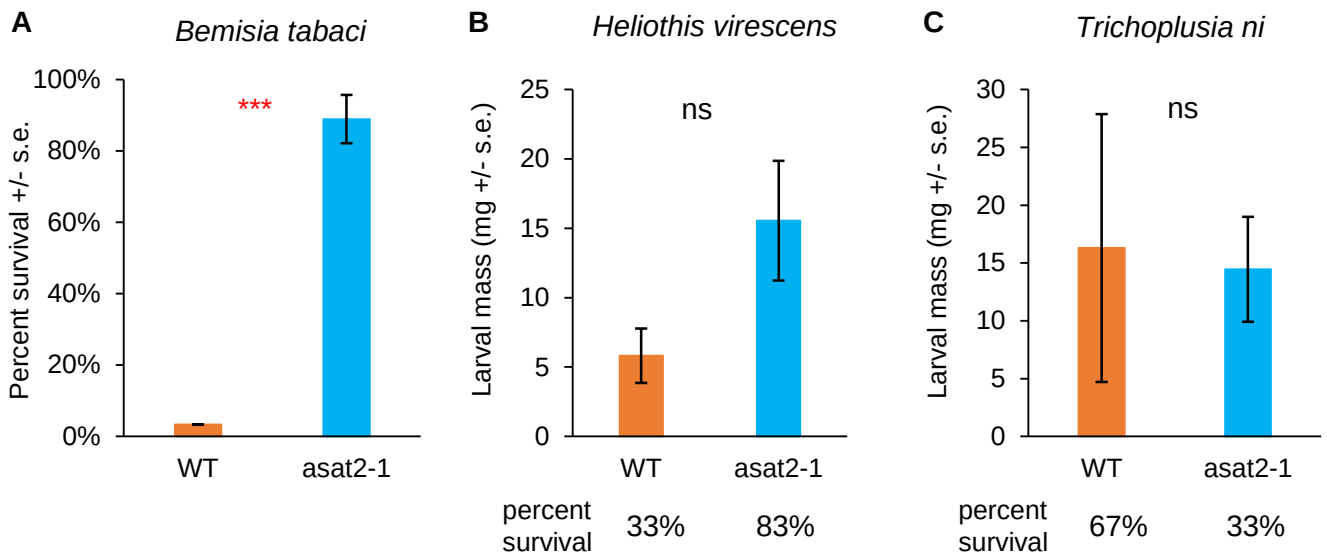

Figure 5. Bioassays of whiteflies and caterpillars on wildtype and *asat2-1* mutant *N. benthamiana*
(A) Whitefly survivorships after 3 days, *** $p < 0.001$, *t*-test. **(B)** Larval mass of surviving *Heliothis virescens* after 10 days of feeding. **(C)** Larval mass of surviving *Trichoplusia ni* after 10 days of feeding. ns: no significant difference ($P > 0.05$, *t*-test).

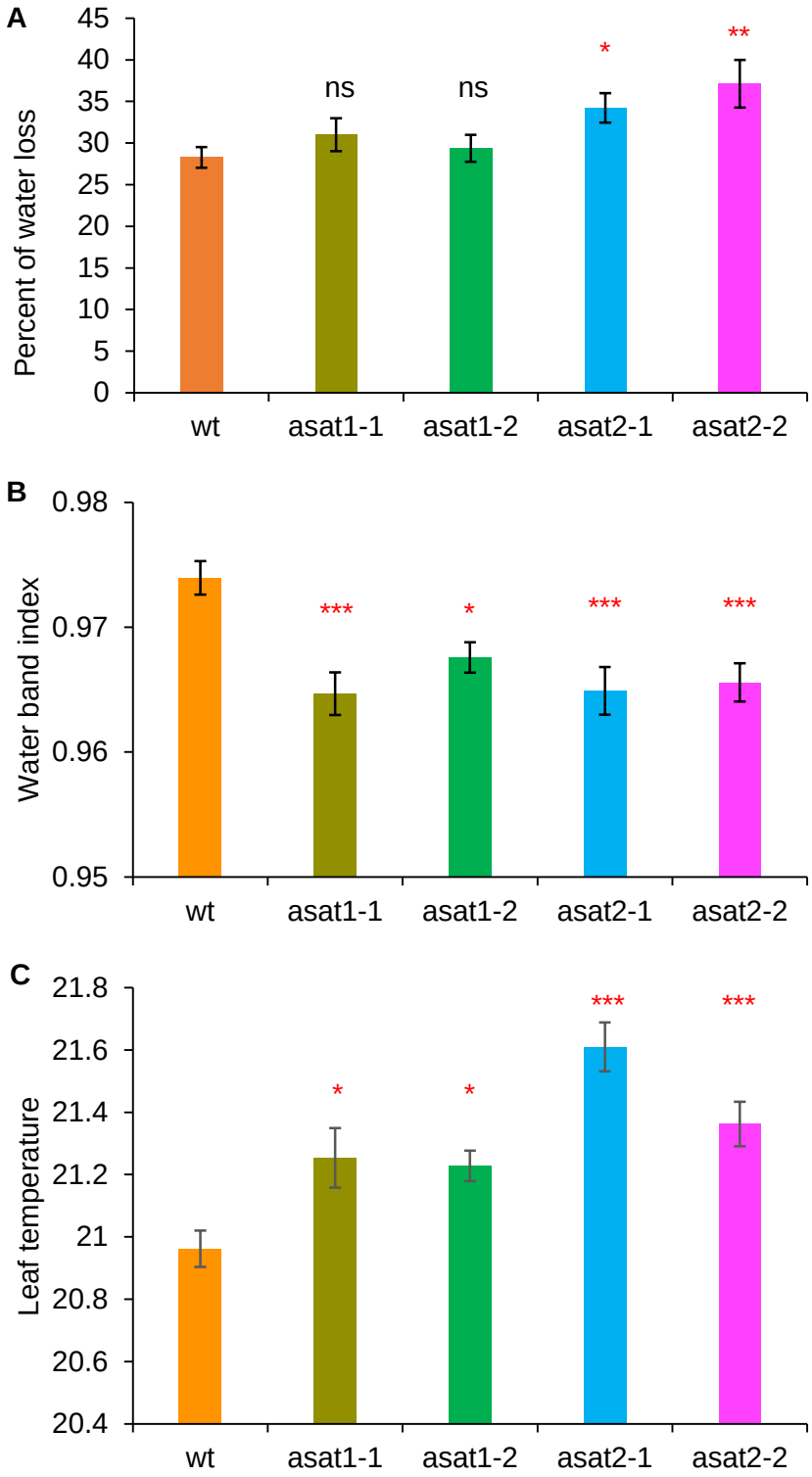

Figure 6. Water loss and leaf temperature of wildtype, *asat1*, and *asat2 N. benthamiana* (A) Percent of water loss from detached leaves in 24 hours (n=15). (**B**) Leaf water content measured by the water band index from hyperspectral imaging (n=20). (**C**) Leaf temperatures from leaves of different plant genotypes (n=20). ns, not significant, *$p < 0.05$, **$p < 0.01$, ***$p < 0.001$, Dunnett's test relative to wildtype control. Error bars = standard error.

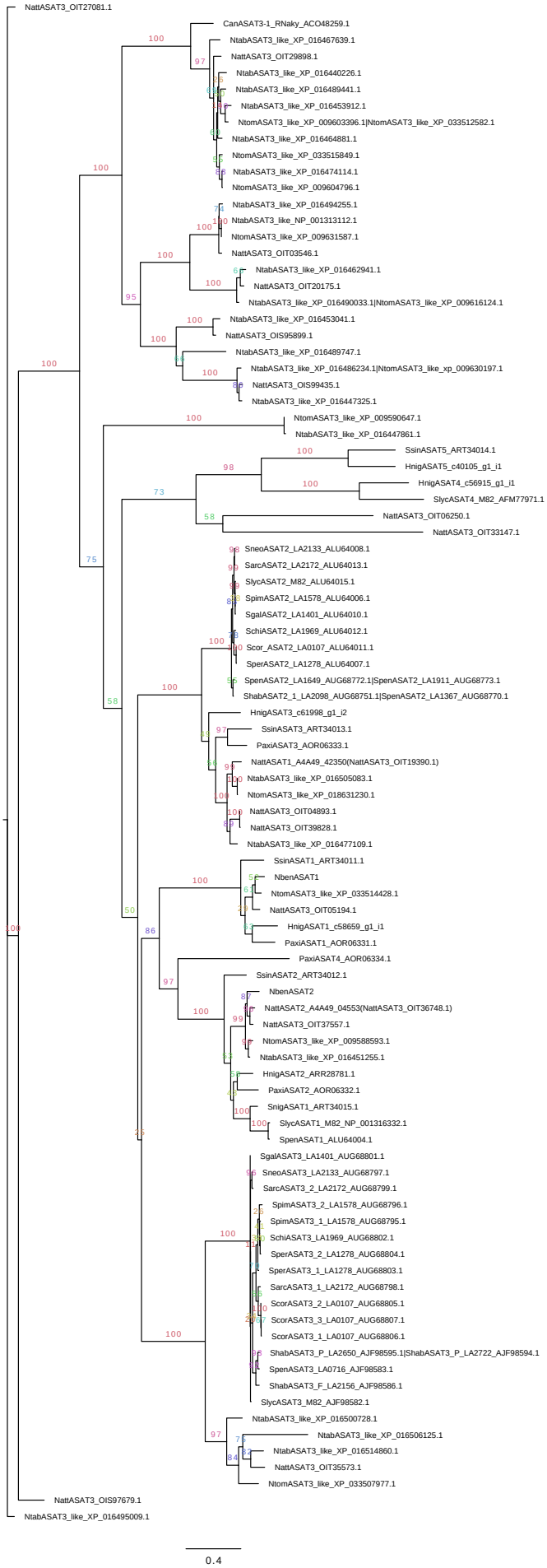

Figure S1. Phylogenetic analyses of annotated ASATs from Solanaceae species

The ASAT proteins used in constructing the tree are listed in Table S1. The evolutionary history of ASATs from Solanaceae species was inferred by using the Maximum likelihood method using RAxML. The branch labels indicated the percentage of trees in which the associated taxa clustered together (bootstrap of 1000).

A

Parent ion *m/z*	MS2 fragment/neutral loss peaks *m/z*	rt*	Annotation
681.34	635.33, 509.22, 491.21, 383.12, 179.06, 143.11, 126.10, 59.01, 18.01	1.76	S3:18(2,8,8) Formate Adduct
671.30	681.34, 671.30, 635.33, 509.22, 143.11, 126.10	1.76	S3:18(2,8,8) Chloride Adduct
635.32	509.22, 491.21, 467.21, 383.12, 365.11, 179.06, 143.11, 126.10, 18.01	1.76	S3:18(2,8,8)
639.32	593.32, 467.21, 449.20, 323.10, 143.11, 126.10	1.70	S2:16(8,8) Intermediate Formate Adduct
593.32	467.21, 323.10, 143.11, 126.10	1.70	S2:16(8,8) Intermediate
667.32	621.31, 509.22, 495.03, 383.12, 179.06, 143.11, 129.09, 126.10, 112.09	1.70	S3:17(2,7,8) Formate Adduct
621.31	495.03, 383.12, 365.11, 143.11, 129.09, 126.10, 59.01, 18.01	1.70	S3:17(2,7,8)
625.31	579.30, 467.21, 453.20, 323.10, 143.11, 129.09, 126.10	1.64	S2:15(7,8) Intermediate Formate Adduct
555.23	509.22, 383.12, 143.11, 126.10, 59.01	1.76	S2:10(2,8) In-Source Fragment Formate Adduct
509.22	449.20, 383.12, 143.11, 126.10, 59.01	1.76	S2:10(2,8) In-Source Fragment
467.21	341.11, 323.10, 144.11, 143.11	1.70	S1:8(8) In-Source Fragment
383.12	383.12, 341.11, 59.01	1.76	S1:2(2) In-Source Fragment

* rt: retention time of the predominant peak for each mass.

B

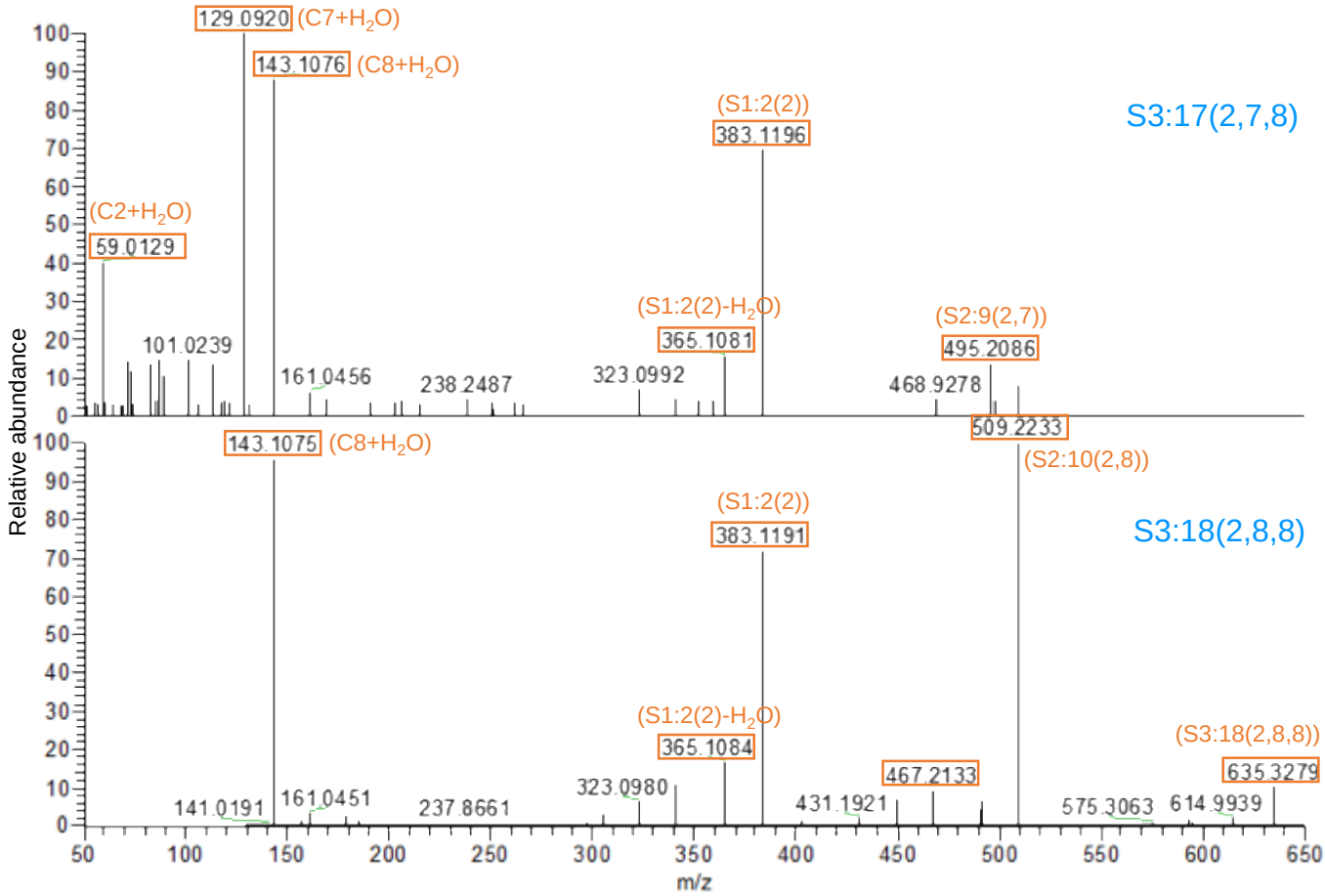

Figure S2 MS/MS chromatography of identified acylsugars

(A) Acyl sugars LC/MS peaks identification and annotation from *N. benthamiana* **(B)** MS^2 chromatography of the two predominant acyl sugars, S2:17(2,7,8) and S2:18(2,8,8). The name of the acylsugars are highlighted in blue and the chromatography is aligned on the x axis based on *m/z*. Highlighted in orange boxes are some of the abundant characteristic mass features and their compositions in parenthesis.

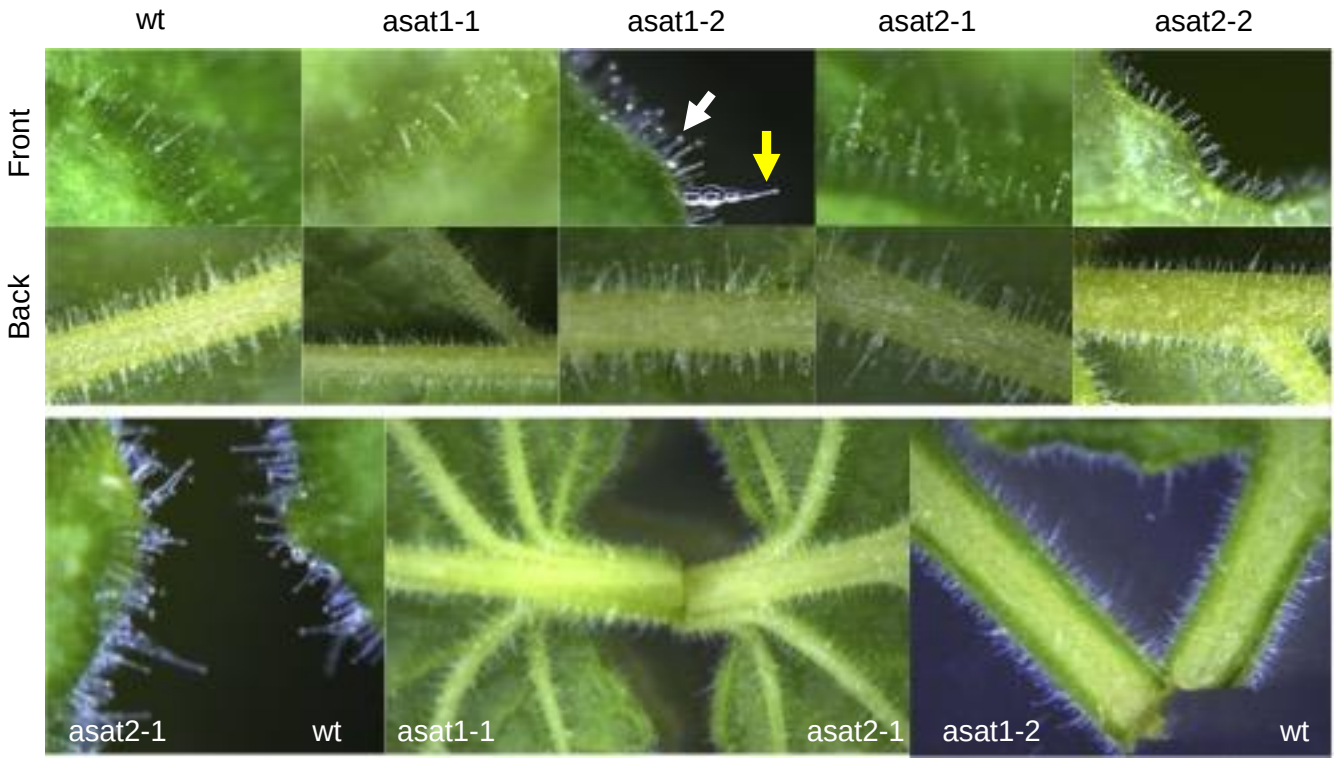

Figure S3. *ASAT* mutations do not affect trichome morphology and abundance
The white arrow indicates the small trichomes and yellow arrow indicates the large swollen-stalk trichomes. Trichome pictures were taken from both the front and back sides of the leaf. Examples of leaves are put side-by-side from different genotypes to facilitate comparisons.

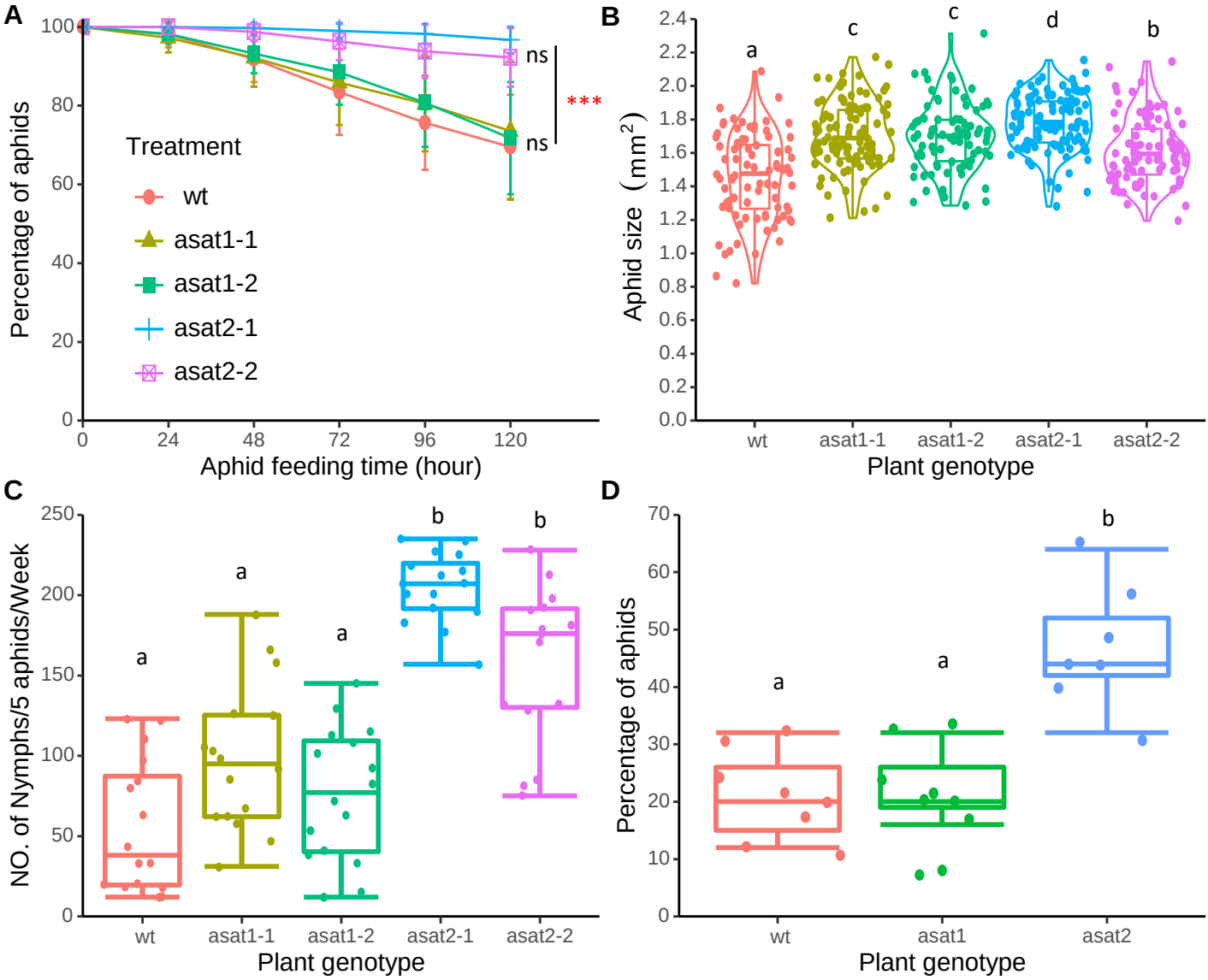

Figure S4. Independent repeat of aphid bioassays shown Figure 4
(A) Aphid survivorship, ns: not significant, *** p<0.001. **(B)** Aphid growth, as measured by aphid body sizes after 120 hours feeding on *N. benthamiana*. **(C)** Aphid reproduction was measured by the number of nymphs that were reproduced by five aphids in a week. **(D)** Aphid choice among detached leaves of each plant genotype. Significant differences between different groups ($p < 0.05$) were determined using ANOVA followed by a Duncan post hoc test and are indicated by lowercase letters above each group in panels B, C, and D.

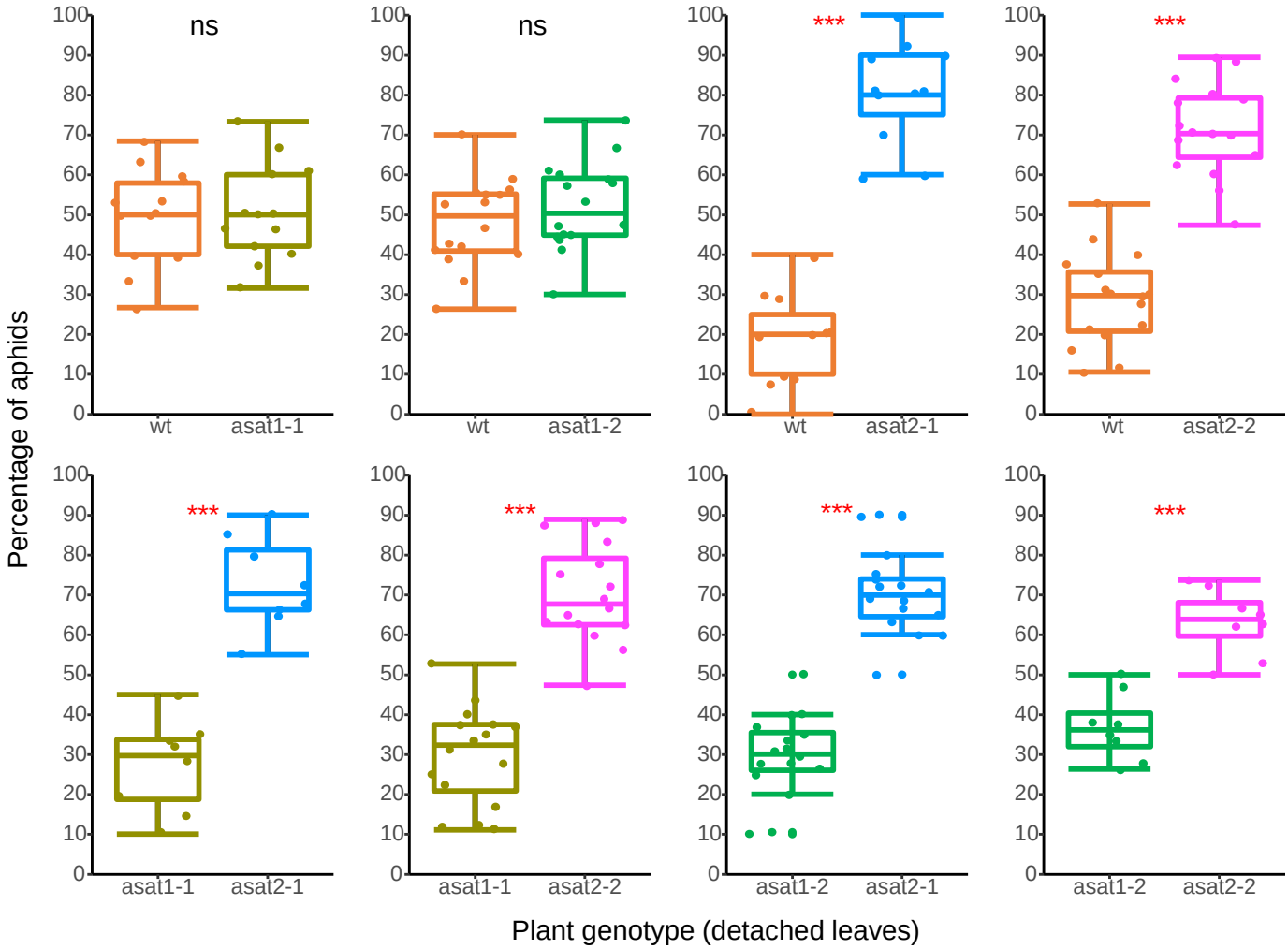

Figure S5. Pairwise aphid choice assay with wildtype and *ASAT* mutant leaves
Each experiment included detached leaves from 5-8 plants of each genotype and was repeated twice with similar results. ***$p < 0.001$, ns: not significant. Significance between different groups were tested using independent samples *t*-tests, error bars = standard deviation.

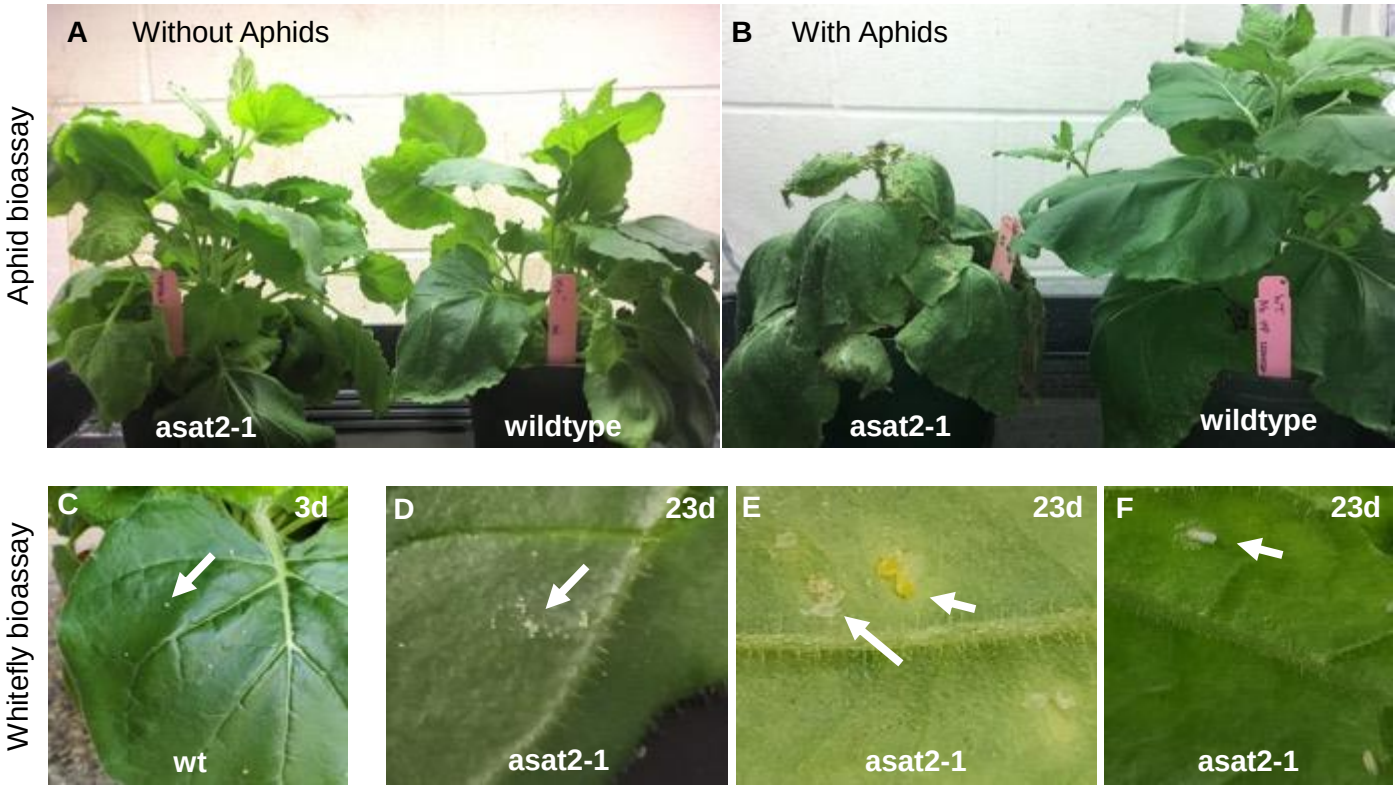

Figure S6. Aphid and whitefly bioassays on wildtype and *asat2-1* mutant *N. benthamiana*
(**A**) without aphid challenge. (**B**) with aphid challenge. One wildtype (right) and one *asat2-1* (left) plant were placed in the same tray in an insect cage. For aphid challenge, ten adult *M. persicae* (from an aphid colony on *N. tabacum*) were released on both the wildtype and the *asat2-1* plants. The picture was taken about one month after the aphid release. Plants in three replications of this experiment looked similar. (**C**) Whiteflies died within three days after release on wildtype *N. benthamiana*. Arrow indicates dead whiteflies. (**D-F**) Whiteflies survived and completed their life cycle on *asat2-1* mutant *N. benthamiana*. At 23 days after release, whiteflies of different life stages were discovered on *asat2-1* mutant plants. Arrows indicate eggs (**D**), eggshells and nymphs (**E**), and adults (**F**).

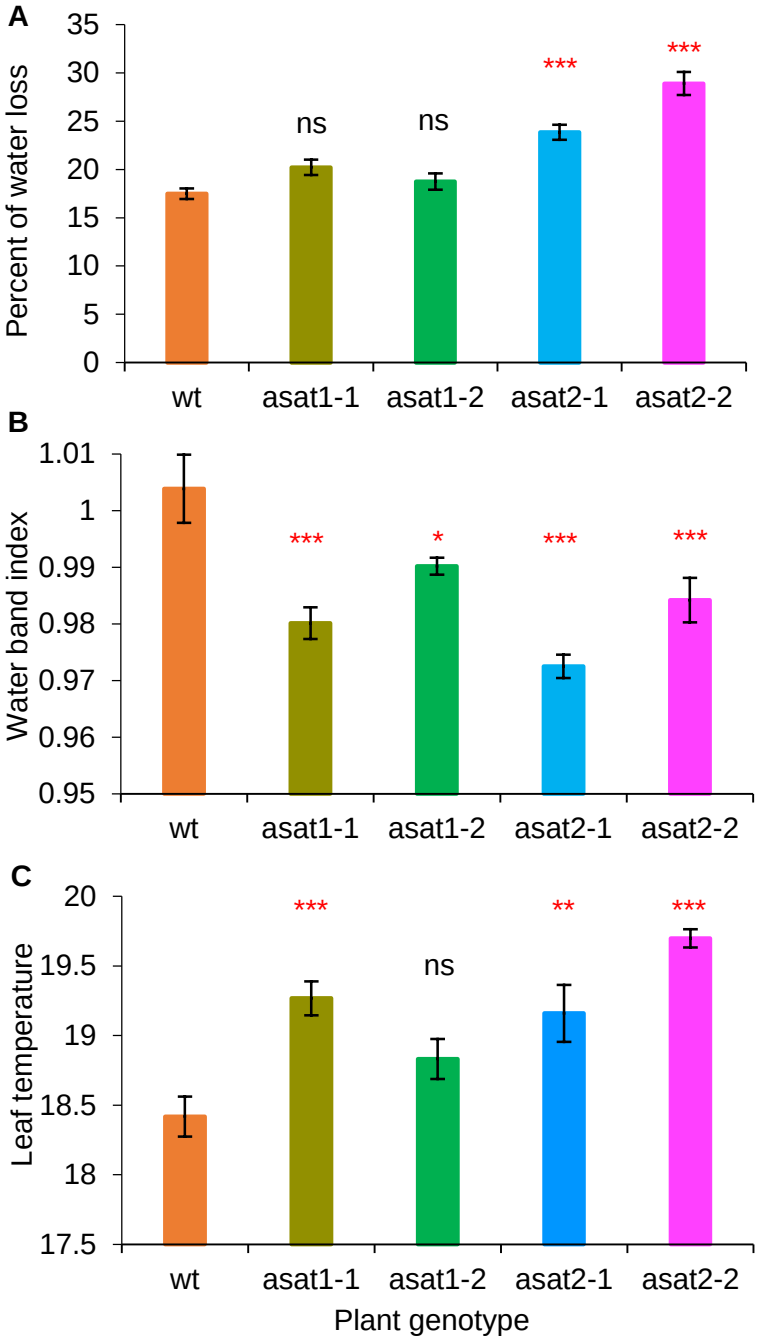

Figure S7. Independent repeat of water loss and leaf temperature shown in Figure 6.
(A) Percent of water loss from detached leaves in 24 hours (n=16). (**B**) Leaf water content measured by the water band index from hyperspectral imaging (n=10). (**C**) Leaf temperatures from leaves of different plant genotypes (n=10 for wildtype and n=5 for mutants). ns, not significant, *p < 0.05, **p < 0.01, ***p < 0.001, Dunnett's test relative to wildtype control. Error bars = standard error.

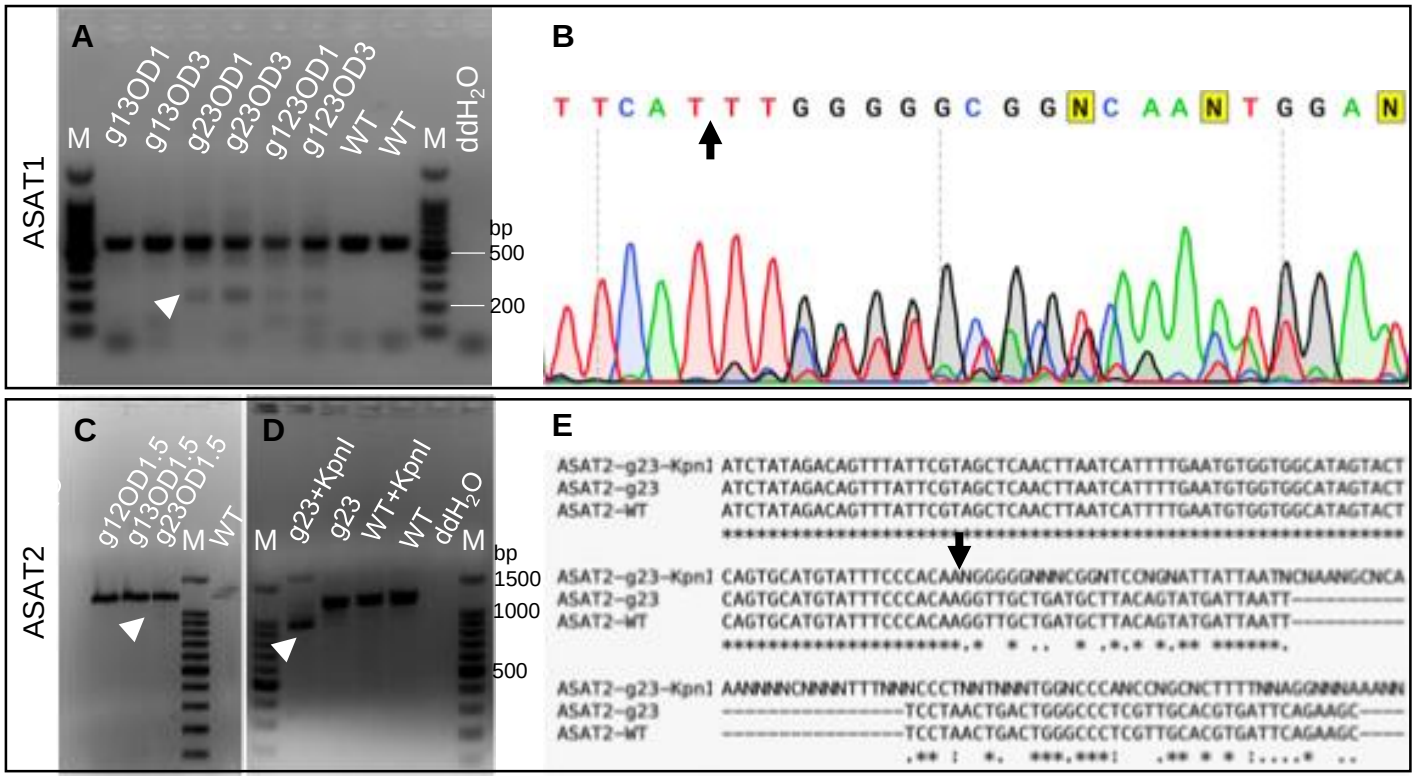

Figure S8. *ASAT* mutagenesis by transiently expressing Cas9 and gRNAs in *N. benthamiana* leaves via agrobacterium infiltration

Three gRNAs each were used for both *ASAT1* and *ASAT2* mutagenesis. (**A**) PCR of plants that infiltrated with combinations of *ASAT1* gRNA constructs. (**B**) DNA sequence confirmation of a representative sample (*i.e.* g23OD3) that displayed a shorter band in panel A. (**C**) PCR of plants that were infiltrated with combinations of *ASAT2* gRNA constructs. (**D**) Restriction enzyme digestion site loss in PCR of g23OD1.5 (from panel C), where, prior to the PCR reaction, genomic DNA was digested with *Kpn*I to remove wild type *ASAT2*. The *Kpn*I restriction site is only present in the expected deletion region. (**E**) Sequence confirmation of sample g23+*Kpn*I from digestion site loss PCR in panel D. Arrow heads indicate the short versions of target genes after a deletion by the two working gRNA constructs. Arrows indicate the positions expected to be cut in gene sequences. The label for each lane in the gel: M, 100 bp DNA marker ladder; WT, samples from wild type plants; ddH2O, no genomic DNA PCR control.

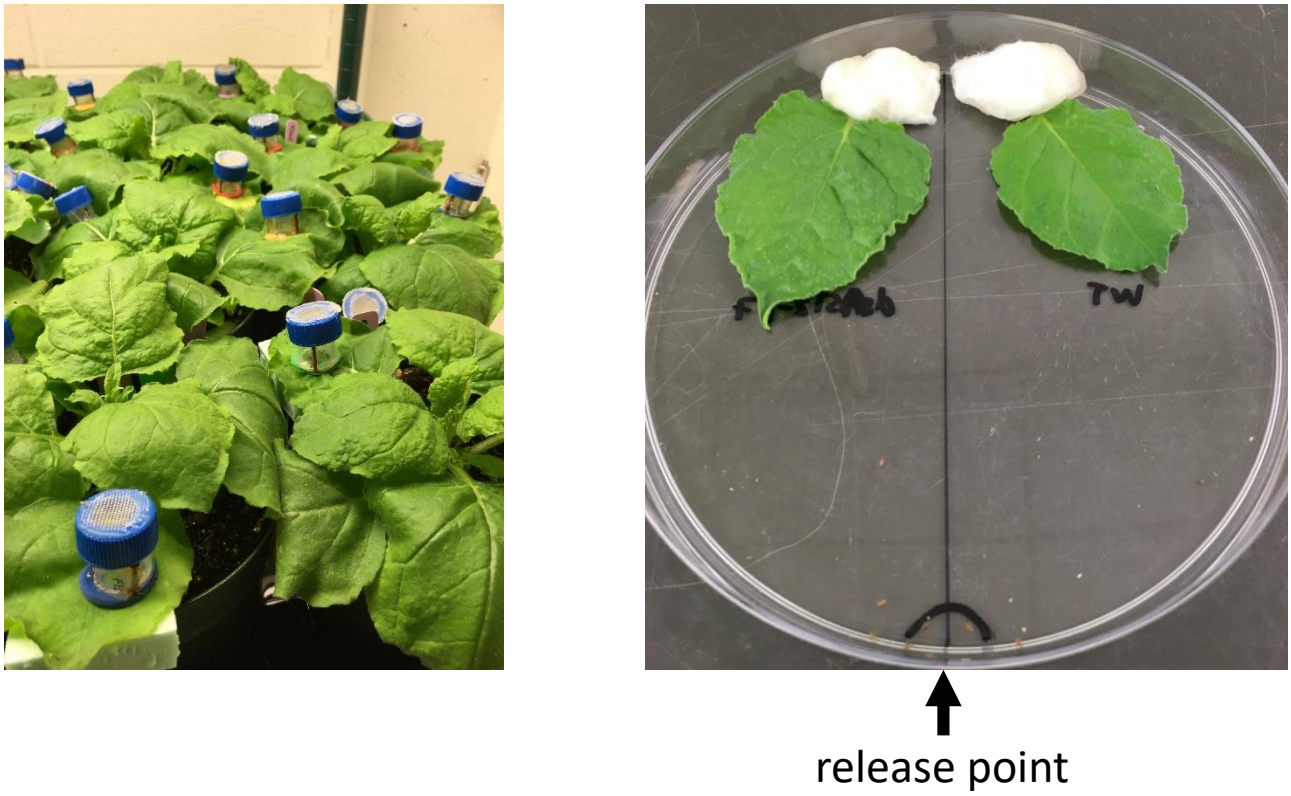

Figure S9. Experimental setups for *Myzus persicae* bioassays
(**A**) Aphid no-choice assays. *Myzus persicae* were caged on individual *Nicotiana benthamiana* leaves. Survival, reproduction, and size were assessed at time points described in the methods section. (**B**) Aphid choice assays. Two *N. benthamiana* leaves were placed in a 15 cm diameter Petri dish with their petioles inserted in moistened cotton swabs, ten *M. persicae* were released into the Petri dish at the indicated position, the dish was covered and placed in complete darkness, and after 24 hours the aphids residing on each leaf were counted